Topographic disequilibrium, landscape dynamics and active tectonics: an example from the Bhutan Himalayas.

Martine Simoes [1], Timothée Sassolas-Serrayet [2], Rodolphe Cattin [2], Romain Le Roux-Mallouf [2,3], Matthieu Ferry [2], Dowchu Drukpa [4]

[1] Université de Paris, Institut de physique du globe de Paris, CNRS, F-75005 Paris, France.
[2] Géosciences Montpellier, Université de Montpellier, CNRS, Université des Antilles, Montpellier, France.
[3] now at Géolithe, 38920, Crolles, France.
[4] Department of Geology and Mines, Thimphu, Bhutan.

Correspondence to: Martine Simoes (simoes@ipgp.fr)

Abstract. The quantification of active tectonics from geomorphological and morphometric approaches commonly implies that erosion and tectonics have reached a certain balance. Such equilibrium conditions are however rare in nature, as questioned and documented by recent theoretical studies indicating that drainage basins may be perpetually re-arranging even though tectonic and climatic conditions remain constant. Here, we document these drainage dynamics in the Bhutan Himalayas, where evidence for out-of-equilibrium morphologies have for long been noticed, from major (> 1 km high) river knickpoints and from high-altitude low-relief regions in the mountain hinterland. To further characterize these morphologies and their dynamics, we perform field observations and a detailed quantitative morphometric analysis using χ plots and Gilbert metrics of drainages over various spatial scales, from major Himalayan rivers to their tributaries draining the low-relief regions. We first find that the river network is highly dynamic and unstable, with numerous evidence of divide migration and river captures. The landscape response to these dynamics is relatively rapid. Our results do not support the idea of a general wave of incision propagating upstream, as expected from most previous interpretations. Also, the specific spatial organization in which all major knickpoints and low-relief regions are located along a longitudinal band in the Bhutan hinterland, whatever their spatial scale and the dimensions of the associated drainage basins, calls for a common local supporting mechanism most probably related to active tectonic uplift. From there, we discuss possible interpretations of the observed landscape in Bhutan. Our results emphasize the need for a precise documentation of landscape dynamics and disequilibrium over various spatial scales as a first step in morpho-tectonic studies of active landscapes.

1 Introduction

The morphology of the Earth's surface and its evolution in space and time result from the competition and balance between tectonics and surface processes. The interplay between these processes, with erosion followed by transport and deposition of the produced sediments in subsiding basins, leads to a continuous dynamic redistribution of masses, eventually modulated by climate (e.g. (Allen, 2008)). In erosive systems, such as in uplifting and growing mountain ranges, such physical

competition between uplift and erosion theoretically leads to steady-state after a characteristic time that mostly depends on the erosional efficiency (e.g. (Whipple and Tucker, 1999;Willett et al., 2001;Bonnet and Crave, 2003;Whipple and Meade, 2004, 2006;Simoes et al., 2010)). This concept of steady-state and equilibrium between tectonics and erosion provides an effective conceptual framework, commonly used for investigating and quantifying active tectonics from geomorphology (e.g. (Lavé and Avouac, 2001)). However, topographic equilibrium may only be reached at a regional scale (Willett and Brandon, 2002), and is expected not to be achieved at the more local scale of the drainage network even though tectonic and climatic boundary conditions remain constant, as illustrated by numerical (e.g. (Sassolas-Serrayet et al., 2019)) or analog (e.g. (Hasbargen and Paola, 2000)) models. The dynamics of the river network are expected to be even more pronounced in natural landscapes for which boundary and forcing conditions vary over time and space. In fact, the formalism used in earlier theoretical studies to model erosion is oversimplified as it does not capture the complex 3D dynamic response of drainage basins, in particular through the constant mobility of drainage divides (e.g. (Goren et al., 2014;Willett et al., 2014)). An example of such landscape dynamics during mountain-building lies in the progressive capture of longitudinal drainages by steeper transverse rivers, as exemplified in the field (e.g. (Babault et al., 2012)) or in analog models (Viaplana-Muzas et al., 2015), or in the dynamic re-organization of the river network as a response to tectonic stresses (e.g. (Castelltort et al., 2012;Guerit et al., 2018)). River captures were also evidenced in old orogens where topographic equilibrium is hypothesized (Prince et al., 2011). This mobility of drainage divides leads to a lengthening of the time needed to reach theoretical steady-state and generates a potential perpetual transience of landscapes (e.g. (Hasbargen and Paola, 2000;Yang et al., 2015;Whipple et al., 2017b)). It is expected to generate variations in the sedimentation rates at river outlets by modifying the sediment routing system (e.g. (Viaplana-Muzas et al., 2019)), and to elucidate observed large dispersions in denudation rates, even in regions that are believed to be in quasi-topographic steady state (Willett et al., 2014;Beeson et al., 2017;Sassolas-Serrayet et al., 2019). Interestingly, this dispersion in measured denudation rates increases most often for smaller drainage basins, further emphasizing that the concept of steady-state is highly scale-dependent as variations related to the local mobility of drainage divides average out at the scale of large river basins (Matmon et al., 2003;Sassolas-Serrayet et al., 2019).

Here, we propose to further investigate these questions, mostly derived from theoretical studies or in few field cases, by considering the emblematic natural example of the Himalayan range in Bhutan (Figure 1). Because of their high rates of continental deformation and erosion, the Himalayas have for long been an ideal natural case for exploring the interactions between tectonics and surface processes, and the associated landscape response (e.g. (Beaumont et al., 2001;Lavé and Avouac, 2001;Burbank et al., 2003;Godard et al., 2004;Hodges et al., 2004;Thiede et al., 2004;Thiede et al., 2005;Grujic et al., 2006;Clift et al., 2010;Adlakha et al., 2013;Godard et al., 2014)). In particular, the Himalayas of Central Nepal have been considered as the archetype of a topography equilibrated on average, from their concave topography and hypsometry (Duncan et al., 2003), or from the observed consistency between denudation (Godard et al., 2014), incision (Lavé and Avouac, 2001) and exhumation (e.g. (Bollinger et al., 2006)) rates over various spatial and temporal scales. Such is not the case further east, in Bhutan, where evidence for out-of-equilibrium morphologies have for long been noticed, from the convex topographic profile (Figures 2a-b), and from high altitude low-relief regions (Figure 1c) and major knickpoints (Figure 2c) within the

mountain hinterland (Duncan et al., 2003;Baillie and Norbu, 2004;Grujic et al., 2006;Adams et al., 2015;Adams et al., 2016). These morphological features have been interpreted in a variety of ways, mostly as reflecting either climatic (Grujic et al., 2006) or tectonic (Baillie and Norbu, 2004;Coutand et al., 2014;Adams et al., 2016) changes, or, in other words, as representing the landscape transience towards a new equilibrium state. However, recent findings in other contexts question these interpretations: low-relief landscapes were shown to form possibly dynamically in-situ as a response to an increase in local base level (e.g. (Babault et al., 2007)), or to a persistent drainage re-organization even in the case of constant tectonics and climate (Yang et al., 2015). Finally, despite these observations in Bhutan and the questions they raise, denudation rates have been considered as reflecting uplift rates and used to derive the geometry of the underlying main active fault (Le Roux-Mallouf et al., 2015) or the timing of interpreted recent tectonic changes (Adams et al., 2016). Whether or not these denudation rates are indeed representative of actual uplift rates needs to be probed. Because smaller drainage basins are the most inclined to have denudation rates deviating from uplift rates in the case of disequilibrium (Sassolas-Serrayet et al., 2019), the answer to this question is intuitively dependent on the size and location of the sampled drainage basins within the overall drainage system.

Figure 1 *(next page)***: Topography, relief and geology of Bhutan.**

a) Geological map of Bhutan, after (Greenwood et al., 2016). Main tectono-stratigraphic units are from south to north: the Gangetic Plain (GP), the Siwaliks Hills (SH), the Lesser Himalayan Sequence (LHS) including the Paro Metasediments (PM) in Western Bhutan, the Greater Himalayan Sequence (GHS) including some leucogranites, and the Tethyan Sedimentary Series (TSS). These units are separated by major tectonic contacts, which are from north to south: the Main Frontal Thrust (MFT), the Main Boundary Thrust (MBT), the Main Central Thrust (MCT), and the South Tibetan Detachment (STD). Locally, some other contacts have been described such as the Kakhtang Thrust (KT) in North-Eastern Bhutan. To the north-west of Bhutan, north of the High Range, the Yadong Rift (YR) is part of the South-Tibetan grabens. The extension of the geological map is reported over the shaded topographic map of Figure 1b.

b) Topographic map of Bhutan, from ALOS World 3D – 30m (AW3D30) DEM data. Main drainage basins are delineated by black lines and associated main rivers are color-coded and labeled. Thick colored lines correspond to the main trunk rivers, while thinner lines indicate main tributaries. Major knickpoints are also reported along trunk and tributary rivers. Dashed rectangles locate the swath profiles of Figures 2a-b. Orange and green arrows on the side of these rectangles locate physiographic transitions T2 and T3 as placed in Figures 2a-b. Inset: Location of topographic map with respect to regional political borders.

c) Map of local relief, as calculated from the topography shown in Figure 1b, with a moving window of 500 m. Major high-altitude low relief areas are manually delineated by dashed red lines. These are from west to east: the Phobijka (PS), the Bumthang (BS), and the Yarab (YS) surfaces. In Western Bhutan, another region of lower relief is also found in the Bhutan hinterland along the Wang and Amo Chhu, even though less well defined than the others: the Wang surface (WS). From west to east, dashed rectangles locate the extension of Figures S4, 9, 7 and S7 (Figures S4 and S7 in supplementary materials).

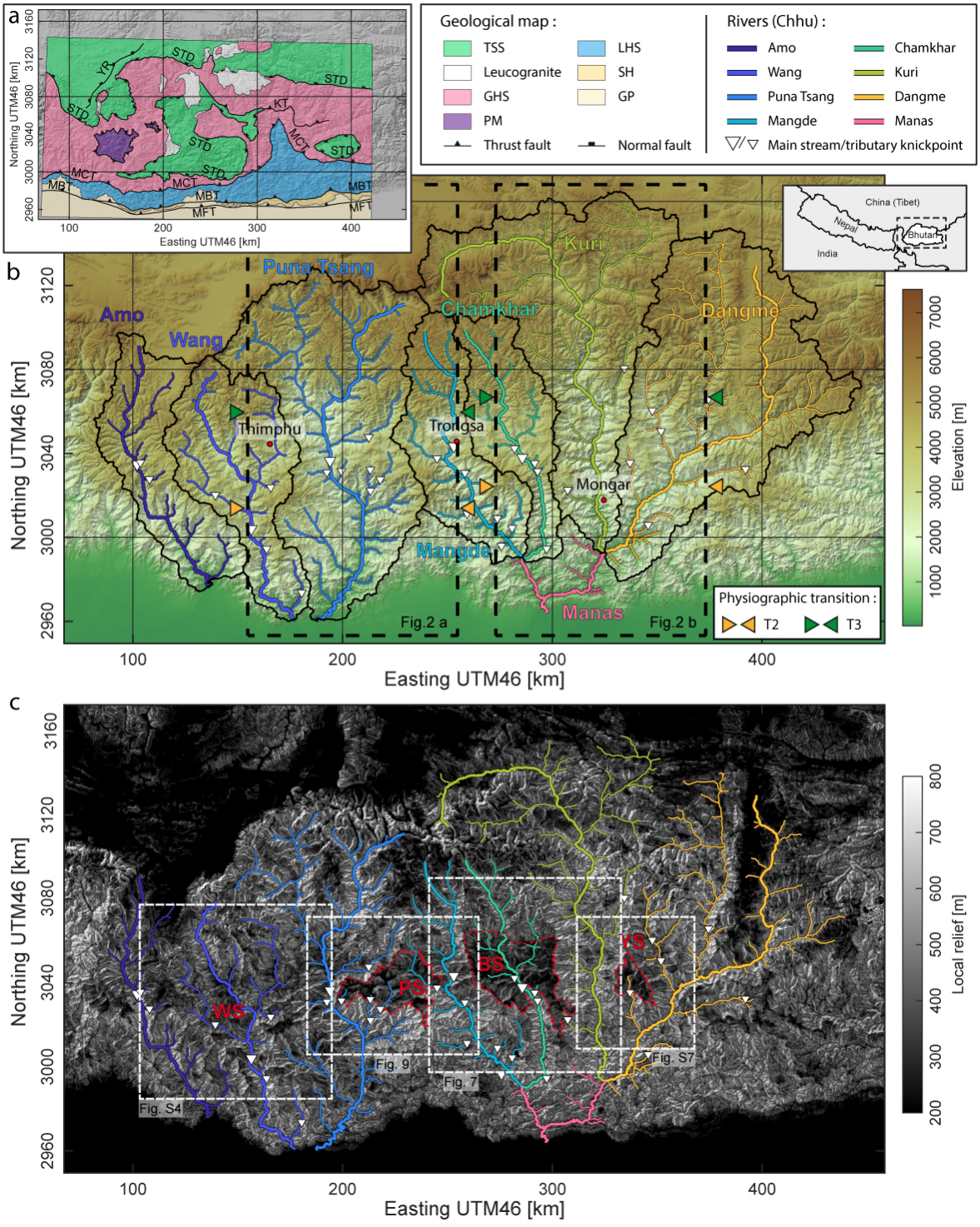
a
Northing UTM46 [km]
Easting UTM46 [km]
STD
YT
KT
MCT
MBT
MFT
Geological map :
TSS
Leucogranite
GHS
PM
Thrust fault
LHS
SH
GP
Normal fault
Rivers (Chhu) :
Amo
Wang
Puna Tsang
Mangde
Chamkhar
Kuri
Dangme
Manas
Main stream/tributary knickpoint
China (Tibet)
Nepal
Bhutan
India
b
Puna Tsang
Amo
Wang
Chamkhar
Kuri
Dangme
Thimphu
Trongsa
Mongar
Mangde
Manas
Fig.2 a
Fig.2 b
Physiographic transition :
T2
T3
Elevation [m]
Northing UTM46 [km]
Easting UTM46 [km]
c
WS
PS
BS
YS
Fig. S4
Fig. 9
Fig. 7
Fig. S7
Local relief [m]
Northing UTM46 [km]
Easting UTM46 [km]

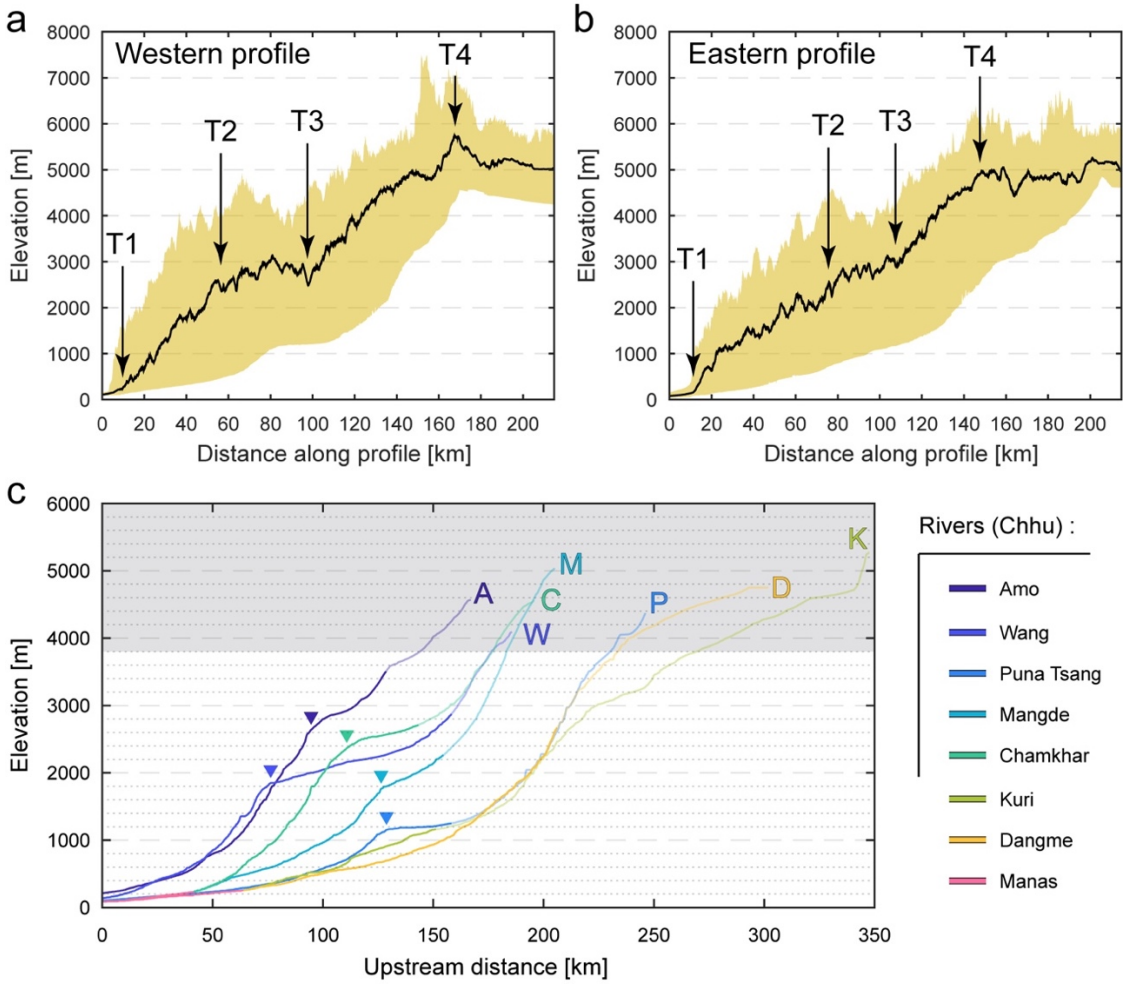

Figure 2: Topographic and longitudinal river profiles.

a-b) Swath topographic profiles across the western (a) and eastern (b) Bhutan Himalayas over a 100 km wide region, from the Gangetic Plain up to the Southern Tibetan Plateau. Location of the swaths is reported in Figure 1b. The colored area encompasses the whole range of altitude values, while the black line draws the median altitude across the profiles. Major physiographic transitions, labeled T1 to T4, are also reported.

c) Longitudinal profiles of major and large rivers in Bhutan, illustrating the variety of river profiles. Rivers are located on the maps of Figure 1, and are here color-coded and labeled. Major knickpoints are also pointed by triangles. Regions with altitudes above 3800 m (grey area) are not to be compared directly to the downstream sections, as these may have a glacial imprint. Portions of the rivers north of physiographic transition T3 are reported by transparent segments. A: Amo Chhu; M: Mangde Chhu; C: Chamkhar Chhu; W: Wang Chhu; P: Puna Tsang Chhu; D: Dangme Chhu; K: Kuri Chhu.

To explore the landscape dynamics of the Bhutan Himalayas as well as their spatial and temporal characteristics, we hereafter conduct a detailed morphometric analysis of this particular field example. We use χ plots (Perron and Royden, 2013) and Gilbert metrics (Whipple et al., 2017b;Forte and Whipple, 2018) for drainages of various dimensions, from major Himalayan rivers to more local tributary streams draining high-altitude low-relief regions. Our analysis does not reveal any evidence for a general wave of incision migrating upstream the drainage network. Instead, we find ample evidence for a high unstability of the river network at various spatial scales that has not been documented yet, with migrating drainage divides and numerous captures. The co-location and spatial organization of all geomorphic features along a longitudinal swath, whatever the considered spatial scale and the dimensions of the investigated drainage basins, calls for a common local origin and support of the observed landscape dynamics, most probably related to active uplift in the mountain hinterland as proposed in some earlier studies. Finally, we discuss the implications of our findings, in particular in terms of how elevated low-relief regions may have formed and in terms of relative time scales of landscape response to network re-organizations.

2 Geological and geomorphological background

2.1 Geological setting

One of the main characteristics of the Himalayan arc is its structural and tectono-stratigraphic continuity over c.a. 2500 km (e.g. (Gansser, 1964, 1983;McQuarrie et al., 2008)). From south to north, and therefore from the Gangetic Plain in the foreland to Southern Tibet, major tectonic contacts are: the Main Frontal Trust (MFT), the Main Boundary Thrust (MBT), the Main Central Thrust (MCT) and the South Tibetan Detachment (STD). The un-metamorphosed synorogenic detrital series of the Siwaliks Group (e.g. (Gautam and Rösler, 1999;Coutand et al., 2016)) are thrusted over the Gangetic Plain along the MFT, which stands as the southern deformation front of the orogen. The Lesser Himalayan series are thrusted over the Siwaliks molasses along the MBT. These series are formed of metasediments, initially deposited on the Indian margin during the Proterozoic and Paleozoic (e.g. (Upreti, 1999;Long et al., 2011b) and references therein), and subsequently deformed, metamorphosed and exhumed since the Mid-Late Miocene, mostly in the form of duplexes in the mountain hinterland (e.g. (Schelling and Arita, 1991;DeCelles et al., 2001;Huygue et al., 2001;Robinson et al., 2001;Bollinger et al., 2004;Bollinger et al., 2006;Long et al., 2012)). Further north, the Greater Himalayan Sequence is thrusted over the Lesser Himalaya along the MCT. This sequence is constituted of granulites and ortho- and para-gneisses of the former Indian margin, with widespread leucogranites (e.g. (Le Fort et al., 1987;Guillot and Le Fort, 1995)). The MCT stands as a thick top-to-the-south shear zone, active by Early to Mid-Miocene (e.g. (Tobgay et al., 2012) and references therein), and subsequently deformed by the duplexes of the Lesser Himalayan series. Finally, the Tethyan Sedimentary Sequence is formed of the sedimentary cover of the northern Indian margin (e.g. (Liu and Einsele, 1994)); it is separated from the high-grade Greater Himalayan rocks by the top-to-the-north normal STD. Except for the un-metamorphosed Siwaliks, the erodability of the series present throughout the mountain range is found to be relatively comparable (Lavé and Avouac, 2001)(Adams et al., 2020).

The Bhutan Himalayas obey this general tectonic and stratigraphic organization observed throughout the Himalayan arc (Figure 1a), even though presenting some peculiarities and specificities (Gansser, 1983;Long et al., 2011a;Greenwood et al., 2016). In particular, the Greater Himalayan and the Tethyan Sedimentary Sequences are here much more exposed throughout the mountain belt when compared to the Himalayas of Central Nepal where these sequences are only preserved in the form of individual klippen (e.g. (Duncan et al., 2003)). In turn, Lesser Himalayan series mostly crop out along the main topographic mountain front, or within structural windows, such as the Paro window in western Bhutan (Tobgay et al., 2012) or the larger Lesser Himalayan window along the Kuri Chhu in eastern Bhutan (Long et al., 2011b) (Figure 1a). Because of the limited flexural subsidence in the broken foreland of Bhutan (Verma and Mukhopadhyay, 1977;Hammer et al., 2013), most probably related to the presence of the Shillong Plateau basement high further south (e.g. (Biswas et al., 2007;Clark and Bilham, 2008;Yin et al., 2010)), the Siwaliks series is here much less developed than elsewhere along the Himalayan arc (Hirschmiller et al., 2014), and the MFT is even absent in western Bhutan (Long et al., 2011a;Greenwood et al., 2016) (Figure 1a).

All major thrust faults are interpreted to branch off the Main Himalayan Thrust (MHT) at depth, which stands as the main crustal-scale detachment at the base of the Himalayan orogenic wedge (e.g. (Schelling and Arita, 1991;DeCelles et al., 2001)). Overall, the geometry of the MHT appears quite simple, with the frontal emerging ramp of the MFT, rooting at depth into a wide shallowly north-dipping structural flat, and pursuing northward down to a mid-crustal ramp beneath the high mountain range. This general structure has been proposed throughout the Himalayas, in particular in Nepal (e.g. (Lyon-Caen and Molnar, 1983, 1985;Schelling and Arita, 1991;Lavé and Avouac, 2001;Bollinger et al., 2004)) but also more recently suggested in Bhutan, as imaged from geophysics (Diehl et al., 2017;Singer et al., 2017), or evidenced from the modeling of interseismic strain (Marechal et al., 2016), thermochronological data (Coutand et al., 2014) or denudation rates (Le Roux-Mallouf et al., 2015). In the details, the flat structure connecting both the frontal and the mid-crustal ramps could be locally more complex with secondary ramps (e.g. (DeCelles et al., 2001;McQuarrie et al., 2008;Adams et al., 2016;Hubbard et al., 2016)).

The Himalayan range is actively absorbing shortening, with rates increasing eastwards from c.a. 13 mm/yr to c.a. 21 mm/yr along the arc (Stevens and Avouac, 2015). Active tectonics are manifested by numerous historical earthquakes all along the Himalayan arc in addition to paleoseismological evidence of major earthquakes rupturing the MHT up to the surface (e.g. (Bilham, 2019) and references therein). Even though much less investigated, the Bhutan Himalayas are also seismically active (Drukpa et al., 2006). They have been struck by a major historical earthquake in 1714 (e.g.(Hetenyi et al., 2016)), in addition to other past events recently revealed in geomorphological and paleoseismological studies along the frontal MFT-MBT thrust system (Berthet et al., 2014;Le Roux-Mallouf et al., 2016;Le Roux-Mallouf et al., 2020).

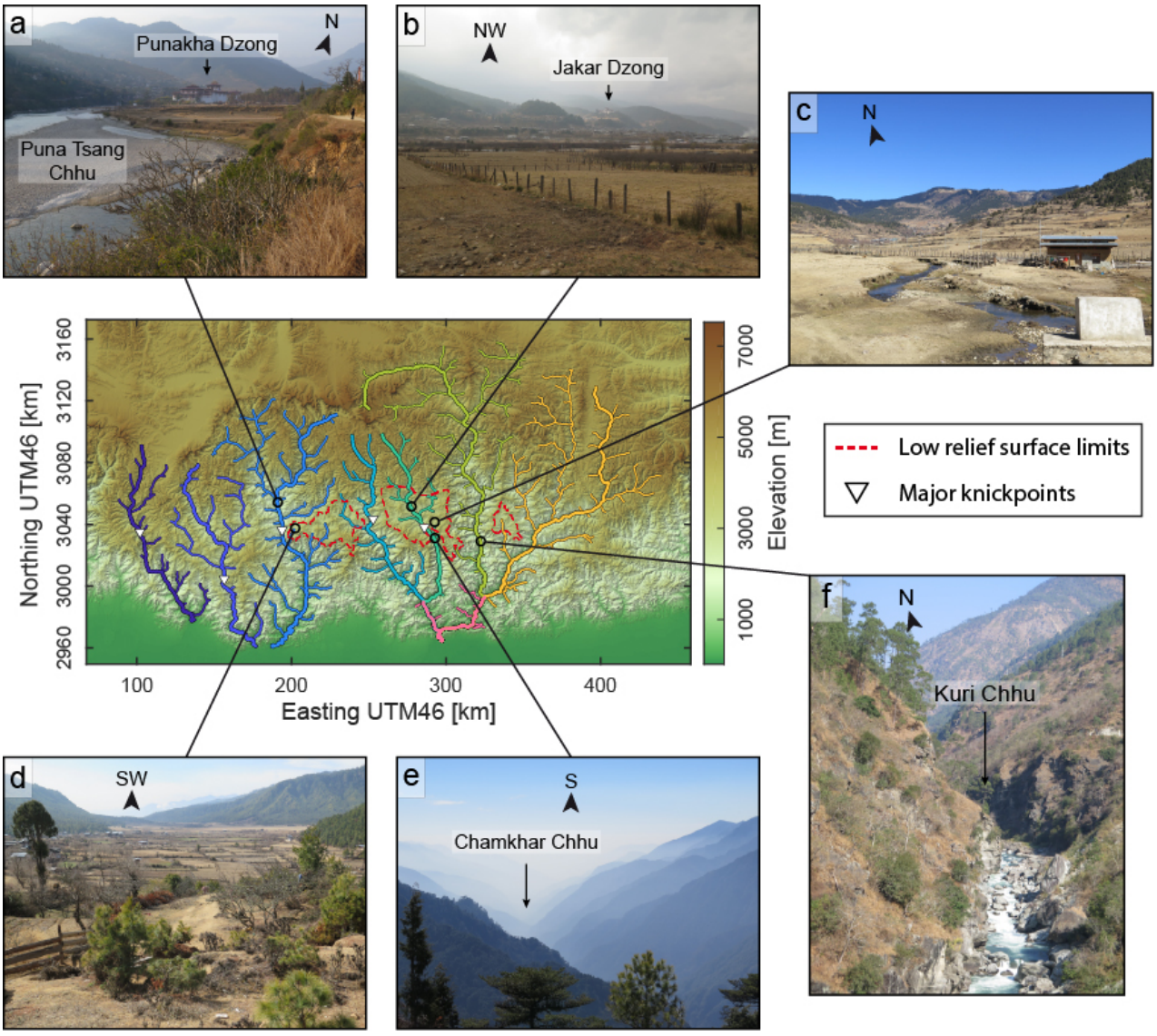

Figure 3: Field pictures representative of the various landscapes in the hinterland of the Bhutan Himalaya.

Topographic map in the center locates field pictures relative to low-relief regions (contoured with red dashed line) and to major knickpoints along rivers (rivers color-coded as in Figures 1-2).

a) Alluvial plain along the PunaTsang Chhu, upstream of its major knickpoint. Picture taken nearby the Dzong of Punakha.

b) Alluvial plain along the Chamkhar Chhu (Bumthang surface), upstream of its major knickpoint. Picture taken nearby Jakar.

c) High-altitude low-relief area of Ura (south-easternmost portion of the Bumthang surface).

d) High-altitude low-relief area of Kotakha (westernmost portion of the Phobijka surface).

e) Deep gorge south of the major knickpoint along the Chamkhar Chhu.

f) Canyon along the Kuri Chhu.

2.2 Geomorphology of Bhutan: general characteristics

The topography of the Bhutan Himalayas is characterized by a convex profile, with four major physiographic transitions, hereafter referred to as T1 to T4 from south to north (modified after (Duncan et al., 2003;Baillie and Norbu, 2004;Adams et al., 2013)) (Figures 2a-b). The first one (T1) corresponds to the rise of the mountain topographic front above the Indo-Gangetic Plain. Northward, topography increases continuously up to c.a. 3000 m on average for the first c.a. 70-80 km (T2), then remains constant on average and high, increases again after c.a. 100-125 km (T3) and reaches average values of c.a. 5000 m by c.a. 175 km (T4) and northwards (Figures 2a-b). Except for T2, these physiographic transitions are also observed in Central Nepal, where the abrupt topographic rise between T3 and T4 has been interpreted as related to the uplift of the High Himalayan range above the mid-crustal ramp of the MHT (e.g. (Lyon-Caen and Molnar, 1983, 1985;Cattin and Avouac, 2000;Lavé and Avouac, 2001;Bollinger et al., 2006)). This interpretation is also expected to hold in Bhutan, as this elevation ascent coincides spatially with the location of the recently evidenced mid-crustal ramp (Coutand et al., 2014;Marechal et al., 2016;Diehl et al., 2017;Singer et al., 2017) - or possibly slightly deported south of this ramp (Le Roux-Mallouf et al., 2015).

The abrupt topographic rise from T1 to T2 and the high-altitude region between T2 and T3 are mostly specific to the landscape of the Bhutan Himalaya along the Himalayan arc (Duncan et al., 2003;Adams et al., 2013). The region between T2 and T3 is characterized by a locally relatively lower relief (Figures 1c and 3a-d), in contrast to what is observed further south from T1 to T2 (Figures 3e-f) but also further north from T3 to T4 where high elevation crests are flanked by deep gorges (Duncan et al., 2003;Baillie and Norbu, 2004;Grujic et al., 2006;Adams et al., 2015;Adams et al., 2016) (Figure 1). More precisely, these lower relief regions may correspond either to high-elevation regions around low-relief alluvial valleys drained by major rivers (ex: the Wang and Bumthang regions traversed by the Wang and Chamkhar Chhu, respectively) (Figures 1c and 3a-b), or to smaller elevated low-relief landscape patches connected to the main drainage network through tributary streams (ex: Phobijkha or Yarab surfaces) (Figures 1c and 3c-d). These valleys or surfaces are characterized by well-developed soils with saprolite horizons, and locally contain bogs (Baillie et al., 2004;Adams et al., 2016). It should be noted that high-elevation low-relief alluvial valleys found along some of the Himalayan rivers (Figures 3a-b) act as local base levels for upstream erosion.

Major rivers in Bhutan have their sources along the southern flank of the high Himalayan peaks, except for the trans-Himalayan Kuri and Dangme Chhu to the east, and to some extent the Amo Chhu to the west, whose headwaters locate within Southern Tibet. These rivers are characterized by a variety of profiles (Baillie and Norbu, 2004), but most of them have significant knickpoints, in some cases of the order of - or higher than - c.a. 1 km (Figure 2c). These knickpoints occur at the head of gorges flowing through low-relief landscapes or immediately downstream of them (Baillie and Norbu, 2004;Adams et al., 2016) (Figures 1 and 3e). They separate rivers in two main segments (Figure 2c): river profiles are steep downstream of these knickpoints, while upstream river portions have alluvial fills (Figures 3a-b) and locate in the low-relief portions of the mountain range, north of T2.

Present-day glacial valleys and cirques are mostly restricted to altitudes higher than c.a. 4200 m (Iwata et al., 2002), and are generally located either nearby T2 or mostly north of T3. Glaciers likely advanced and expanded to altitudes of c.a. 3800 m during the Holocene and Pleistocene (Iwata et al., 2002;Meyer et al., 2009). There is no evidence for glacial imprint on the high-altitude low relief landscapes investigated here, except locally along some of the southern edges of low relief areas where altitudes reach c.a. 4000 m (Adams et al., 2016).

2.3 Geomorphology of Bhutan: previous interpretations

By comparing the morphology and geology of these two regions of the Himalaya, (Duncan et al., 2003) proposed that topographic and morphologic differences between Central Nepal and Bhutan could be related to an along-strike tectonic segmentation of the Himalayan range and to the associated variable balance between uplift and erosion, in which the timing of large-scale deformation and uplift would be younger in Bhutan. This interpretation of a less mature landscape would be supported by the extensive exposure of Great Himalayan and Tethyan sequences in Bhutan (e.g. (Gansser, 1983;Long et al., 2011a;Greenwood et al., 2016)) (Figure 1a), which contrasts with the klippen of Central Nepal (e.g. (Gansser, 1964;Schelling and Arita, 1991;DeCelles et al., 2001;Bollinger et al., 2004)). Lateral variations in the timing of major fault systems along the Himalayan arc cannot be excluded, such as for the Main Central Thrust by the Early to Mid-Miocene (e.g. (Tobgay et al., 2012) and references therein) or for the exhumation of the Lesser Himalayan sequences since the Late Miocene (e.g. (Huygue et al., 2001;Robinson et al., 2001;Bollinger et al., 2006;Long et al., 2012) and references therein). However, such interpretation would first require that the large-scale landscape response time be much greater than what could be justifiable given the regional high erosion rates (e.g. (Lavé and Avouac, 2001)). Also, in this case, erosion rates in Bhutan would be expected to have increased in recent geological times, as a response to balance uplift. However, thermochronological data rather suggest a general decrease in exhumation rates over the last 4-6 Myr (Grujic et al., 2006;Coutand et al., 2014;Adams et al., 2015).

This general decrease in exhumation rates since Late Miocene - Early Pliocene has been invoked by (Grujic et al., 2006) to be related to the rainshadow generated by the coeval topographic rise of the Shillong Plateau further south in the foreland of Bhutan (e.g. (Biswas et al., 2007;Clark and Bilham, 2008;Govin et al., 2018;Rosenkranz et al., 2018) and references therein). Such rainshadow would have led to lower erosion rates, and from there to locally increased relief and elevation by modifying the balance between uplift and erosion. Following this idea, high altitude low-relief regions in Bhutan would be relict landscapes of prior wetter conditions. However, as noticed by (Baillie and Norbu, 2004), the rainshadow by the Shillong Plateau is relative as climatic conditions are everywhere wet and tropical in Bhutan (Bookhagen and Burbank, 2006). Some variations exist along the foothills, with modern precipitation rates peaking to more than 6 m/yr on average in between physiographic transitions T1 and T2, but climatic conditions are then relatively constant northward within the range interior (north of T2). Also, low-relief regions are mostly found within the western half of Bhutan (Figure 1c), where the Shillong rainshadow is supposedly lowest or inexistent according to (Grujic et al., 2006).

In addition to these general observations on the overall topography or the presence of low-relief areas in the range interior, (Baillie and Norbu, 2004) noticed the variety of river profiles (Figure 2c), despite overall similar climatic and

lithologic conditions along Bhutan, and from there suggested that these morphologies be mostly related to lateral differential tectonics, accommodated by north-south faulting. However, such laterally variable uplift should produce a significant along-strike variability in exhumation rates, a pattern not seen in thermochronological data (Grujic et al., 2006;Coutand et al., 2014;Adams et al., 2015). Indeed, most significant variations in exhumation rates are across-strike and not along-strike, and should relate to cross-sectional changes in the geometry of the underlying Main Himalayan Thrust (Coutand et al., 2014;Le Roux-Mallouf et al., 2015).

More recently, (Adams et al., 2015) found that the decrease in exhumation rates since 4-6 Ma retrieved from thermochronology is observed everywhere in Bhutan, within or outside a supposed rainshadow, and proposed that it reflects a southward transfer of deformation towards the Shillong Plateau. Morphological characteristics in Bhutan are here interpreted as a recent local rejuvenation of the landscape related to uplift in the mountain hinterland that would not have yet produced sufficient exhumation to be recorded in cooling ages. Based on the observation that large rivers are over-steepened between physiographic transitions T1 and T2 (Figure 2c) and that most of these rivers develop alluvial plains upstream of T2 (Figures 3a-b), these authors proposed that major convex knickpoints and upstream low-relief regions around alluvial valleys are the geomorphic response to the uplift related to a local blind duplex in the Bhutan hinterland (Adams et al., 2016). This interpretation also relies on the similarity between these observations and the results of a numerical landscape evolution model (after (Tucker et al., 2001)) in which rivers adjust to higher uplift rates in the hinterland of a mountain range by aggrading upstream of convex knickpoints. Major knickpoints are interpreted by (Adams et al., 2016) as migrating upstream and upwards, and while so as removing packages of fill deposits in the upstream alluvial valleys. Within this framework, low-relief regions are interpreted as remnants of formerly incising valleys that were filled in-situ with sediments while locally uplifted. From there, they are used to derive the amount of uplift with respect to a theoretical initial river profile, and the timing of the tectonic perturbation (Adams et al., 2016). Using denudation rates measured from in situ produced cosmogenic isotopes in river sands, within and outside the low-relief areas, (Adams et al., 2016) suggest that this rejuvenation is c.a. 0.8-1 Ma old. Even though the idea of localized uplift over a blind ramp is seducing, some details in their interpretation need further investigations. Indeed, given the variety of river profiles in Bhutan (Figure 2c), the choice of the river impacts the amount of uplift derived by comparing the present profile with a theoretical one. Also, using differential denudation rates to determine the timing of uplift implies that these are representative of uplift rates, an assertion that may not be valid in a setting where the landscape is inevitably out-of-equilibrium (e.g. (Sassolas-Serrayet et al., 2019)).

Previous interpretations have therefore attributed the specificities of the morphology of the Bhutan Himalayas (by contrast to that of Central Nepal), to changes in either climatic or tectonic boundary conditions. They rely on the idea that high-altitude low-relief regions are either uplifted relict landscapes or remnants of formerly incising valleys that have been filled in-situ while uplifted, and imply that major knickpoints reflect a general transient wave of incision migrating upstream into the drainage system. These various assertions on the dynamics of the river network still need, however, to be clearly documented and explored to verify or refine these interpretations.

3 Data and Methods

Field observations within the hinterland of Bhutan are complemented by a morphometric analysis of the landscape dynamics, further detailed hereafter. Field work was conducted during two two-weeks long campaigns in January-February 2015 and in February 2017.

3.1 Topography: data and analytical tools

Our study relies on topographic data obtained from the ALOS World 3D – 30m (AW3D30) Digital Elevation Model (DEM) provided by the Japanese Aerospace Exploration Agency. It has been shown that this DEM has the highest precision when compared to other DEMs with equivalent resolution so that it is well suited to the analysis of river profiles in high relief regions (Schwanghart and Scherler, 2017). For our analysis, we use the Matlab-based function library TopoToolbox, which provides essential tools for large scale geomorphological approaches, including drainage network and watershed extraction, or computation of usual river or topography metrics (Schwanghart and Scherler, 2014). For additional information, in particular on the various algorithms of the library used hereafter, the reader is referred to the TopoToolbox documentation (https://topotoolbox.wordpress.com) and to the references provided therein.

Topographic relief is determined as the difference between maximum and minimum altitudes in a sliding window of 500 m radius so as to get a fine resolution on this metrics. Even though we extract morphometric parameters along the whole drainage network, we specifically focus on the region south of the High Himalayan peaks, i.e. south of physiographic transition T3, where the fluvial network is supposedly the least affected by a potential glacial imprint (altitudes < 3 800 m) and where morphological features characteristic of disequilibrium (major knickpoints, elevated low-relief regions) have been described.

3.2 Drainage network analysis

3.2.1 Drainage network extraction and pre-processing

To extract the hydrographic network, we use the Single Flow Direction algorithm (SFD) implemented in TopoToolbox, from which an accumulation map is computed. This accumulation map provides the drainage area upstream each pixel of the DEM, and from there allows to choose the network extension by defining a threshold source area. We extract the river network with a minimal drainage area of 50 km^2. This systematic extraction avoids the manual *ad-hoc* selection of specific rivers, which could otherwise bias the analysis.

We extract the main river systems of the Bhutan Himalaya upstream of the topographic front (T1). This supposes that the Gangetic plain is taken as the base level of the extracted upstream drainage network. In Eastern Bhutan, major river confluences occur just upstream the deformation front: indeed, the Manas Chhu forms downstream of the confluence of the four Mangde, Chamkhar, Kuri and Dangme Chhu transhimalayan rivers from west to east, respectively (Figure 1). In this

specific case, we individualize these river systems upstream of their confluences to improve the clarity of the figures and to facilitate their comparison.

Once the river network is extracted, we erase small scale topographic noise associated with DEM artifacts along river paths using the Constrained Regularized Smoothing (CRS) algorithm (see (Schwanghart and Scherler, 2017) for further details). Smoothing parameters are carefully selected by cross-checking so as to remove erratic noise while keeping real topographic features such as knickpoints that may be present along river profiles. Here, we use a smoothness (parameter K in CRS algorithm) of 3.5, and a a quantile carving (parameter τ in CRS) between 10 and 90. The use of smoothed river profiles allows for an easier extraction of knickpoints. It also allows for a more accurate computation of some stream metrics (gradient, steepness...).

3.2.2 Extraction of knickpoints

Knickpoints are automatically detected using the Knickpointfinder algorithm implemented in TopoToolbox (Schwanghart and Scherler, 2014). As for the smoothing of river profiles, detection parameters are refined by cross-checking, and a tolerance value of 50 is used. The final knickpoints list is then manually corrected. We do not consider knickpoints above altitudes of 3800 m as these may be mostly due to glacial or post-glacial morphologies. We also manually remove doubtful minor knickpoints most probably associated with imperfect local smoothing. This method does obviously not give an exhaustive list of knickpoints along Bhutanese rivers, but it ensures the retrieval of large knickpoints and of their spatial organization as needed for our study.

3.2.3 Computation of transformed coordinates (χ)

The computation of χ transformed river coordinates has proved useful for the understanding of landscape and drainage network dynamics (e.g. (Perron and Royden, 2013;Willett et al., 2014;Yang et al., 2015;Whipple et al., 2017b)). In this coordinate system, the elevation z at a given position along the river bed x depends of the integral quantity χ following equation (1):

$$z(x) = z(x_b) + \left(\frac{U}{K{A_0}^m}\right)^{\frac{1}{n}} \chi \quad (1)$$

with

$$\chi = \int_{x_b}^{x} \left(\frac{A_0}{A(x)}\right)^{\frac{m}{n}} dx$$

where x_b locates the channel outlet; $A(x)$ is the drainage area upstream of the position x along the channel; A_0 is a reference scaling area; m and n are constant empirical parameters most often expressed as the m/n ratio. This ratio can be related to the reference concavity index θ_{ref} that describes how the river gradient evolves along the river profile. Such integral approach is based on the stream power equation of river incision (e.g. (Howard, 1994;Whipple and Tucker, 1999)). It provides a simple metric for pointing out and analyzing variable forcing conditions or the nature of transient signals within the river network, by

comparing trunk streams and their tributaries in profiles corrected for their variable upstream drainage areas - and therefore their variable spatial scales - (Perron and Royden, 2013) (Figure 4).

Figure 4 *(next page)***: Schematic river profiles and metrics expected in the case of equilibrated rivers, of a wave of incision migrating upstream the river network, or of stream piracy and divide migration.**

a) Longitudinal (left) and χ (right) profiles of a main trunk river (dark line) and its tributaries (grey lines) in the case that these rivers are in equilibrium with external forcing conditions that are constant over the whole area. The χ profiles of these various rivers are here all linear (constant forcing conditions) and colinear (same forcing conditions), within a certain variability related to natural conditions (Perron and Royden, 2013).

b) Longitudinal (left) and χ (right) profiles of a main trunk river (dark line) and its tributaries (grey lines) in the case of the migration of a wave of incision through the river network. Knickpoints are present along the various streams at variable locations, but their χ profiles are all concordant, within the variability due to natural conditions (Perron and Royden, 2013).

c) χ profiles expected in the case of migrating divides (left) or river captures (right). Aggressor (or pirate) stream is represented in red, and the victim in blue. The dark line represents the profile expected for rivers equilibrated with external forcing. Area gain shifts the χ profiles of aggressor streams to lower χ values, above the equilibrium line. Conversely, area loss shifts the χ profiles of victim streams to higher χ values, below the equilibrium line. Here, χ profiles are discordant (Willett et al., 2014).

d) Assessment of divide migration and its direction from the across-divide contrast in χ (Willett et al., 2014) (left) or in Gilbert metrics such as local slope or relief (Whipple et al., 2017b;Forte and Whipple, 2018) (right).

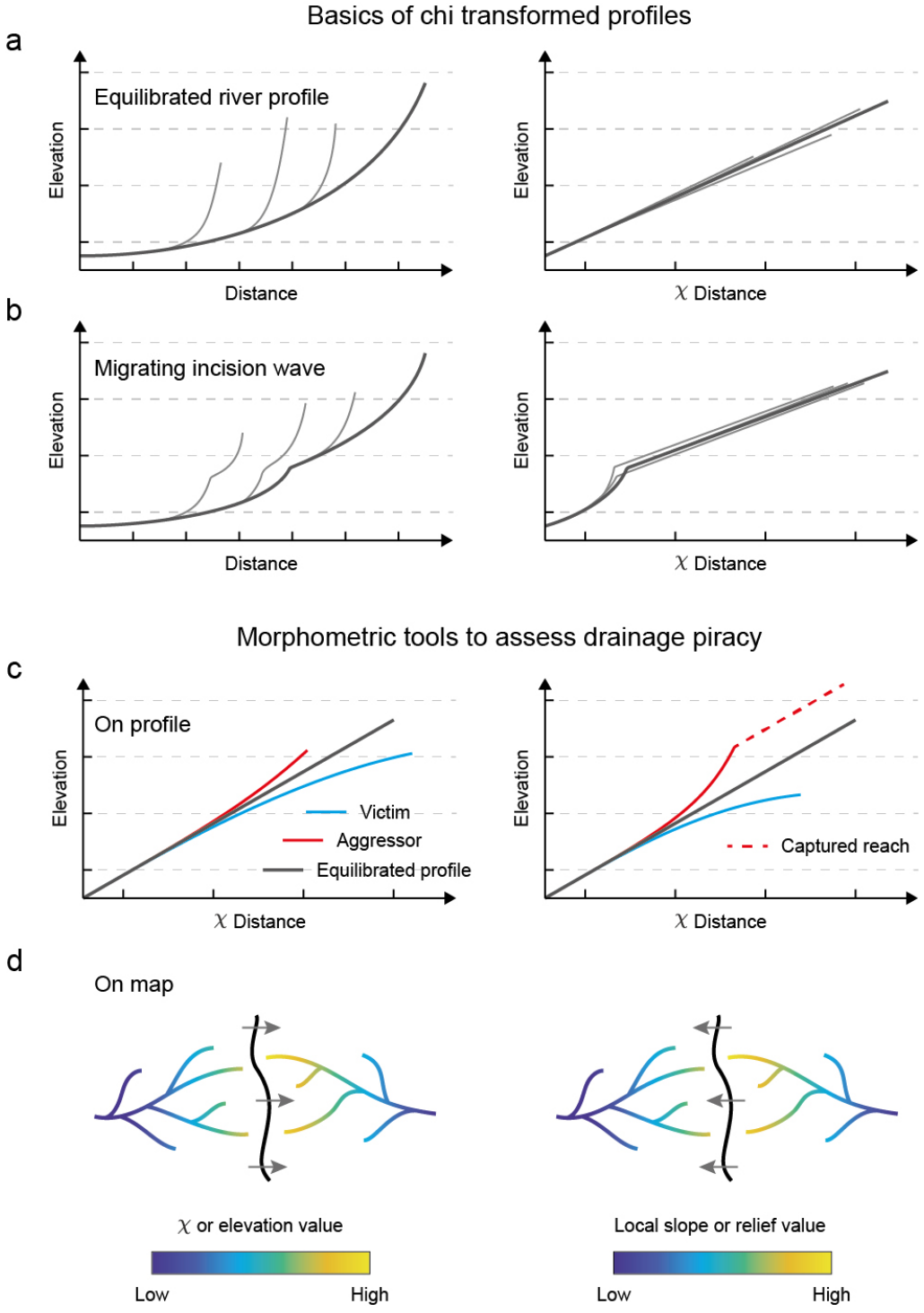
Basics of chi transformed profiles
a
Equilibrated river profile
Elevation
Distance
Elevation
χ Distance
b
Migrating incision wave
Elevation
Distance
Elevation
χ Distance
Morphometric tools to assess drainage piracy
c
On profile
Elevation
Victim
Aggressor
Equilibrated profile
χ Distance
Elevation
Captured reach
χ Distance
d
On map
χ or elevation value
Low
High
Local slope or relief value
Low
High

370

The χ plot of an equilibrated concave river system obeying the stream power equation, with uniform conditions, is a straight line along which both main trunk stream and tributaries collapse (Figure 4a). Furthermore, by setting A_0 to unity, the slope of the χ profile is equal to the channel steepness K_{sn} (Perron and Royden, 2013). This metric is linked to the uplift rate U and the erodibility coefficient K, by the equation:

$$K_{sn} = \left(\frac{U}{K}\right)^{\frac{1}{n}} \quad (2)$$

For U and K varying along the profile of the river, steeper (gentler) segments in χ profiles relate either to locally higher (lower) uplift rate or to lower (higher) erodibility. However, any assessment of these parameters from river profiles is not direct and straightforward as they depend on parameter n, which is not known a priori (e.g. (Mudd et al., 2018)). In the following, we assume that there is no significant variation in the erosion processes over the study region. Also, we do not consider a specific value for n and use $\theta_{ref} = 0.5$ (see supplementary material, in which the effect of the chosen concavity index is tested for θ_{ref} ranging between 0.3 and 0.7). Such assumptions allow for a relative comparison between the various parts of the drainage network over our study area.

3.2.4 Assessment of the drainage network dynamics

We use transformed χ profiles to detect and analyze perturbations within the river network. Knickpoints in longitudinal profiles of main trunk and tributaries that migrate upstream following a wave of incision in response to a common change in forcing or boundary conditions are expected to cluster and be concordant in transformed coordinates (Perron and Royden, 2013) (Figure 4b). Conversely, migrating knickpoints of differing origins (ex: local discrete river captures) will be discordant both in longitudinal and χ profiles. In the case of migrating knickpoints, whether concordant or discordant in χ coordinates, the river steepness around knickpoints is representative neither of the actual local uplift rate nor of the erodibility, but rather of the upstream migration of an incision wave. Spatially fixed knickpoints, as a response to local variations in uplift or erodability, are expected to be also discordant in transformed coordinates.

Transformed χ plots are also useful to unravel drainage reorganization related to migrating divides and river captures (Willett et al., 2014). A river capture leads to a characteristic χ profile (Willett et al., 2014) (Figure 4c). Indeed, an abrupt increase in drainage area due to a capture shifts the profile of the pirate stream to lower χ values, i.e. above a theoretical equilibrium profile. Conversely, area loss shifts the profile of the victim stream to higher χ values, i.e. below a theoretical equilibrium profile (Figure 4c). χ profiles of rivers affected by captures are therefore expected to be discordant, transiently after the capture and before re-equilibrating to the new boundary conditions. This is also expected for migrating divides without discrete captures (Yang et al., 2015), unless the response of channels to drainage area changes is faster than that of divide migration (Whipple et al., 2017b). Such signatures of captures or area loss by piracy in transformed coordinates are defined relatively to an equilibrium river profile, specified theoretically or in the field from equilibrated trunk or major rivers.

It should be noticed that a certain degree of discordance in transformed χ profiles is acceptable given the variabiity of natural conditions, even in the case of equilibrated rivers or in the case of rivers responding to a common wave of incision (Figures 4a-b). We choose not to define quantitatively what could be taken as an acceptable degree of discordance in river profiles as it implies to specify a threshold that is by essence arbitrary. This will not affect our results and conclusions as major knickpoints in Bhutan are largely dispersed and discordant in χ, amplitude and altitude.

We also use maps of χ along the drainage network to detect potential migrating divides, and to assess the direction of these migrations. A contrast in the value of χ across a divide results in its migration toward the stream with the highest χ (Willett et al., 2014) (Figure 4d). Recent studies show, however, that the direction of divide migration interpreted from a χ analysis is not straightforward and can be biased by the assumed river base level (Whipple et al., 2017b;Forte and Whipple, 2018). Spatially variable tectonic or climatic conditions, as well as rock properties, may also maintain χ contrasts across stable divides. To overcome these limitations, we strengthen our analysis of across-divide contrasts by using "Gilbert metrics" associated with contrasts in elevation of the river bed, in mean upstream local slope and in mean upstream local relief at a given drainage reference area (Whipple et al., 2017b;Forte and Whipple, 2018), taken here as 2 km². Migration of the divide is expected to occur towards the stream with relative higher elevation, and conversely with relative lower local slope or relief (Figure 4d).

In addition, we infer divide motion by locating morphological indicators of regressive erosion like beheaded channels (or wind gaps), from Google Earth satellite imagery or field observations. These complementary methods enable a more careful assessment of divide migration direction and drainage network re-organization.

4 Results

4.1 General observations, and definition of the spatial scales of investigation

Based on the visual interpretation of longitudinal and χ profiles, we define three profile types for major rivers in Bhutan (Figures 2c and 5). First, the Kuri and Dangme Chhu in Eastern Bhutan are characterized by concave upward profiles south of the high range (south of physiographic transition T3), with no remarkable major knickpoint. These rivers correspond to the two largest drainage basins, with drainage areas > 9000 km^2 (Table 1). Second, the Amo, Wang and Chamkhar Chhu have major knickpoints (> 1 km high), located approximately nearby T2. These knickpoints separate a steep river segment to the south from a river segment with lower gradient to the north. More specifically, the river portion with lower gradient flows within and across an alluvial plain (Figure 3b) located in a high-altitude low-relief region (Figure 1c). These rivers are those among the major Himalayan rivers of Bhutan with the smallest drainage basins (drainage areas of < 5000 km^2) (Figure 1, Table 1 and Figure S10 in supplementary material). Third, the Puna Tsang and Mangde Chhu have intermediate characteristics: their longitudinal profile is overall concave upward with a more modest (< 1 km high) knickpoint nearby the region of T2, and they flow through a limited (Puna Tsang Chhu - Figure 3a) or inexistent (Mangde Chhu) alluvial plain upstream of this knickpoint.

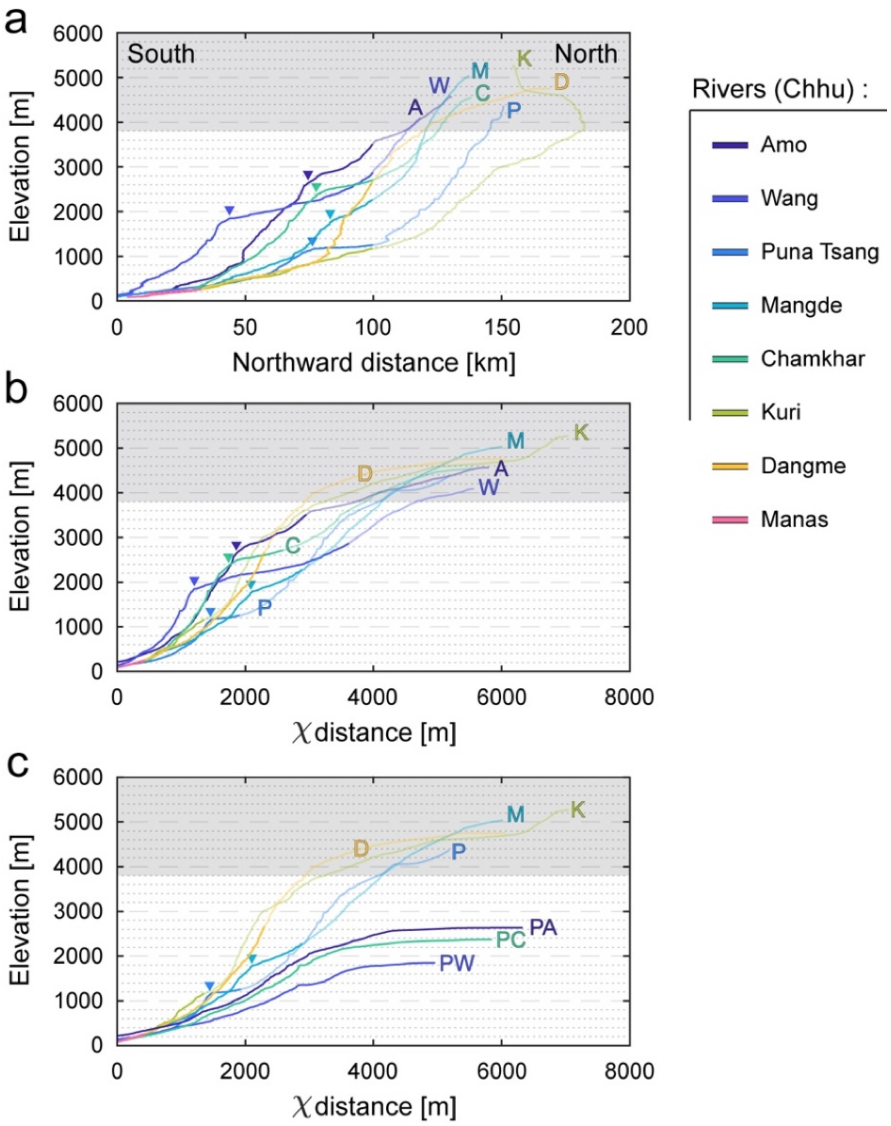

Figure 5: Projected and transformed profiles of major and large rivers in Bhutan. Rivers are located on the maps of Figure 1, color-coded and labeled. Major knickpoints are also pointed by triangles. Regions with altitudes above 3800 m (grey area) are not to be compared directly to the downstream sections as these may have a glacial imprint. Portions of the rivers north of physiographic transition T3 are reported by transparent segments. (P)A: (Proto-)Amo Chhu; (P)W: (Proto-)Wang Chhu; P: Puna Tsang Chhu; M: Mangde Chhu; (P)C: (Proto-)Chamkhar Chhu; K: Kuri Chhu; D: Dangme Chhu.

a) Longitudinal profiles projected along a north-south axis, approximately perpendicular to active tectonic structures and to structural directions (Figure 1a). Except for the Wang Chhu, all major knickpoints are located c.a. 75-80 km north of the mountain front.

b) Transformed river profiles, following the formalism of (Perron and Royden, 2013). The Gangetic Plain is used as the base level for all these rivers. χ transformed profiles are established with a concavity of 0.5 (see Figure S1 in supplementary material for similar transformed profiles but using other concavity values).

c) Theoretical transformed river profiles of the proto-Wang, -Amo and - Chamkhar Chhu, compared to the transformed profiles of other large rivers. Profiles of proto-rivers are determined here by removing all the drainage area upstream of the major knickpoint. A large portion of these theoretical profiles remains relatively flat in transformed coordinates (for χ > c.a. 3000m) as the steepness of these rivers is low nearby their knickpoint (immediately upstream and downstream), over a limited real distance of a few km at most.

Table 1: Drainage areas of large Himalayan rivers in Bhutan, taken upstream of their outlet at the mountain front or upstream of a major confluence.

River	Drainage area (km^2)
Amo Chhu	3752
Wang Chhu	4600
Puna Tsang Chhu	9701
Mangde Chhu [a]	3819
Chamkhar Chhu [a]	3174
Kuri Chhu [b]	9652
Dangme Chhu [b]	10485

[a] The drainage areas of the Mangde and Chamkhar Chhu are here calculated upstream of their confluence.

[b] The drainage areas of the Kuri and Dangme Chhu are here calculated upstream of their confluence.

These major rivers define the local base level for the incision of their tributaries (Figure 6). Longitudinal profiles of tributaries exhibit a great variability relative to their trunk stream (Figure 6a). This variability decreases and specific trends emerge when transformed into χ coordinates (Figure 6b). On one hand, most tributaries appear colinear with their trunk stream in χ plots - at least colinear in χ over comparable spatial regions of the mountain range, in particular at the level of their confluence. On the other hand, some tributaries plot above the trunk stream. These tributaries are characterized by a downstream steep channel and an upstream gentle segment. The gentle segments correspond to high-altitude low-relief patches of the landscape (Figures 1 and 3c-d).

Given the above general observations of major rivers and of their tributaries, we define various scales of investigation of the landscape dynamics in Bhutan. First, we analyze major trunk rivers draining the Bhutan Himalayas and discuss their diversity. Next, we focus on those showing major knickpoints and flowing through alluvial plains in high-altitude low-relief regions of the range. We finally analyze the tributaries of main trunk rivers, in particular nearby perched low-relief regions. For each spatial scale, we describe our results and present the interpretations that can be directly derived from them. We recall that we focus hereafter only on the regions south of physiographic transition T3.

4.2 Major Himalayan rivers

Here, the longitudinal and χ profiles of the Kuri, Dangme, Puna Tsang and Mangde Chhu are discussed and compared (Figures 2c and 5). Except for the Mangde Chhu, these rivers correspond to the largest drainage basins of Bhutan (Table 1).

The two easternmost major rivers (Kuri and Dangme Chhu) show a very similar long river profile, incising deep into the mountain range (Figure 3f) as altitudes of c.a. 2000 m are reached c.a. 200 km from their outlet at the Gangetic Plain (Figure 2c). This is also the case for the Puna Tsang Chhu, c.a. 100-150 km further west in Western Bhutan, which only departs locally from the previous longitudinal profiles by c.a. 130 km from the outlet, at the level of its major - but relatively modest (c.a. 300-400 m high) - knickpoint. The longitudinal profile of the Mangde Chhu is well above that of these other major rivers.

When transformed into χ coordinates, the profiles of these four rivers compare well and are overall colinear within our region of interest south of T3 (Figure 5b). It should be emphasized here that the major knickpoints of the Puna Tsang and Mangde Chhu are not concordant in transformed coordinates, with variable χ and most importantly with altitudes that vary by c.a. 600 m.

These observations suggest that major rivers share and have adjusted overall to similar tectonic and/or climatic forcing conditions in our region of interest, even though located throughout Bhutan (Figure 1).

Figure 6 *(next page)***: Longitudinal (a- top) and transformed χ (b- bottom) profiles of major rivers of Bhutan and of their tributaries** (with drainage area > 50 km2) (location in Figure 1). Major drainage basins (and the corresponding horizontal axes of their profiles) are color-coded as in Figure 1. Trunk streams are reported in bold lines, and tributaries in thinner lines. Lighter transparent colors are used for the river portions north of physiographic transition T3. Major knickpoints are pointed out by triangles. Altitudes above 3800 m are considered aside (grey band) as rivers may preserve a glacial imprint in these regions. χ transformed profiles are established with a concavity of 0.5. Other concavities have been tested and are illustrated in Figure S2 (supplementary material). For an easier reading of the figure, horizontal axes (distance or χ) are alternatively reported below or above the graphs, and follow the same color-code as that of the rivers they are associated to.

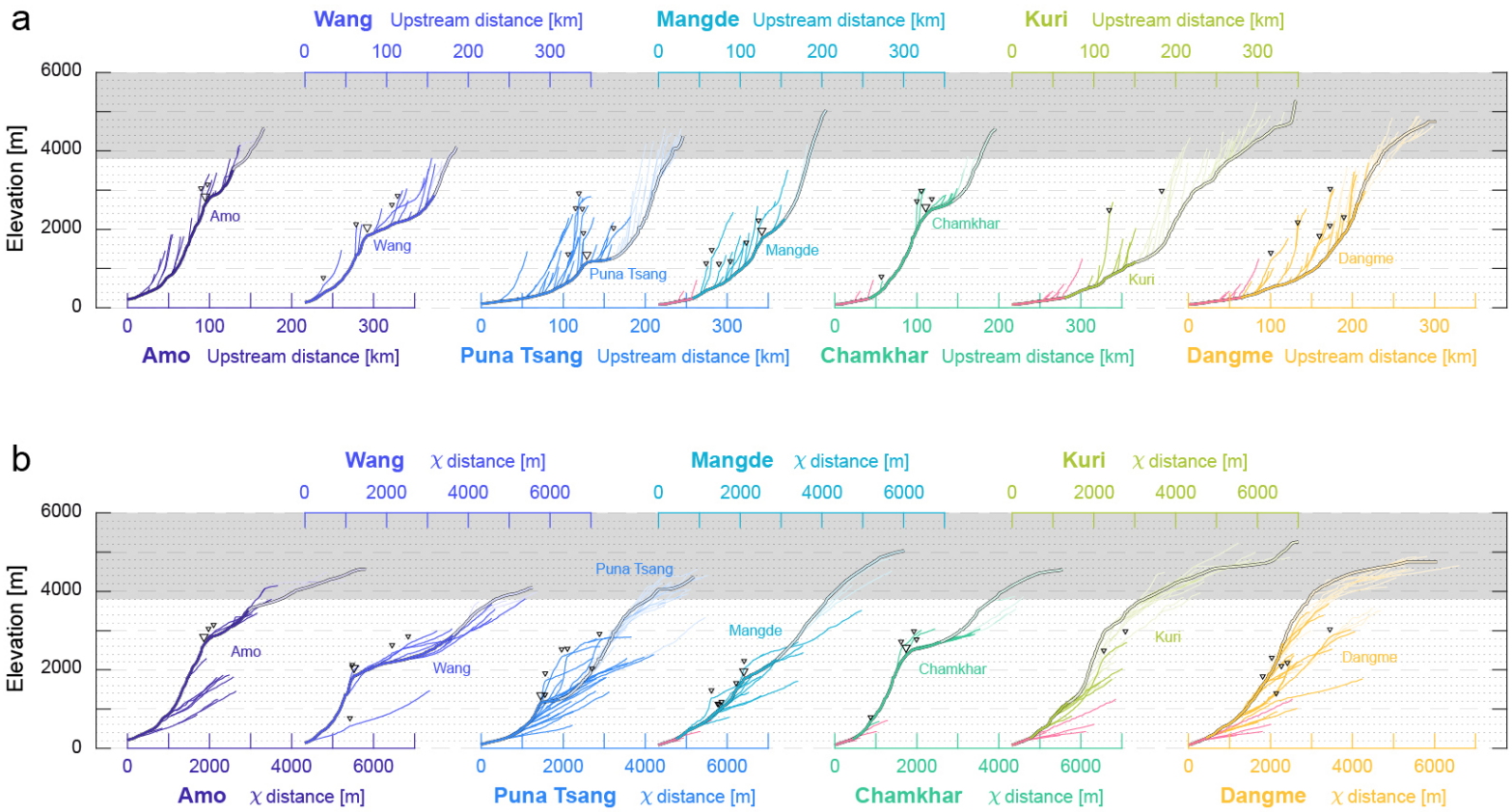
a
Wang Upstream distance [km]
Mangde Upstream distance [km]
Kuri Upstream distance [km]
0 100 200 300
6000
4000
2000
0
Elevation [m]
Amo
Wang
Puna Tsang
Mangde
Chamkhar
Kuri
Dangme
Amo Upstream distance [km]
Puna Tsang Upstream distance [km]
Chamkhar Upstream distance [km]
Dangme Upstream distance [km]
b
Wang χ distance [m]
Mangde χ distance [m]
Kuri χ distance [m]
0 2000 4000 6000
Amo χ distance [m]
Puna Tsang χ distance [m]
Chamkhar χ distance [m]
Dangme χ distance [m]

4.3 Large Himalayan rivers draining low-relief alluvial plains

The Chamkhar, Wang and Amo Chhu have longitudinal and χ profiles that are well above those of the formerly discussed major Bhutanese rivers (Figures 2c and 5b). This is not surprising for longitudinal profiles as these three rivers have more modest drainage areas (Table 1), but this pattern remains even in χ coordinates. It should also be noticed that the profiles of these rivers are not colinear in χ coordinates, with χ values and altitudes of major knickpoints that vary by c.a. 1000 m and by c.a. 1400 m, respectively (Figure 5b).

These rivers are also characterized by the mobility of their drainage divides, as illustrated in Figures 7 and S3 (supplementary material) in the case of the Chamkhar Chhu. As intuitively expected, the high-altitude low-relief Bumthang region traversed by the Chamkhar Chhu is being laterally aggressed by the tributaries of the deeply incising Mangde (to the west) and Kuri (to the east) Chhu. As a result, the main drainage divides around this low-relief region are migrating inwards and drainage area is locally shrinking (Figures 7 and S3). The reverse situation is observed further south, downstream of the major knickpoint of the Chamkhar Chhu. Gilbert metrics suggest that drainage divides are here migrating outwards so that drainage area is locally increasing (Figures 7 and S3). Similar observations and conclusions are reached for the Wang Chhu (Figure S4 in supplementary material), even though the situation of the Wang Chhu is slightly more complex.

Altogether, our results indicate that the Chamkhar Chhu, and possibly the Wang Chhu, flowing through high-altitude low-relief alluvial plains in the hinterland, have overall disequilibrium characteristics. Their χ profiles, well above the regional average defined by the transformed profiles of other major rivers throughout Bhutan (Figure 5b), are possibly indicative of a gain of drainage area by large-scale river captures (see Figure 4c; following (Willett et al., 2014;Yang et al., 2015)). This interpretation is comforted by the fact that the transformed profiles of these rivers get closer to that of other major rivers when corrected for the drainage area upstream of their major knickpoints (Proto-Amo, -Wang and -Chamkhar Chhu in Figure 5c). Additionally, in the details, we find evidence for an ongoing dynamic rearrangement of the river network within these large drainage basins, with a specific pattern of drainage area loss and expansion on either side of their major knickpoint.

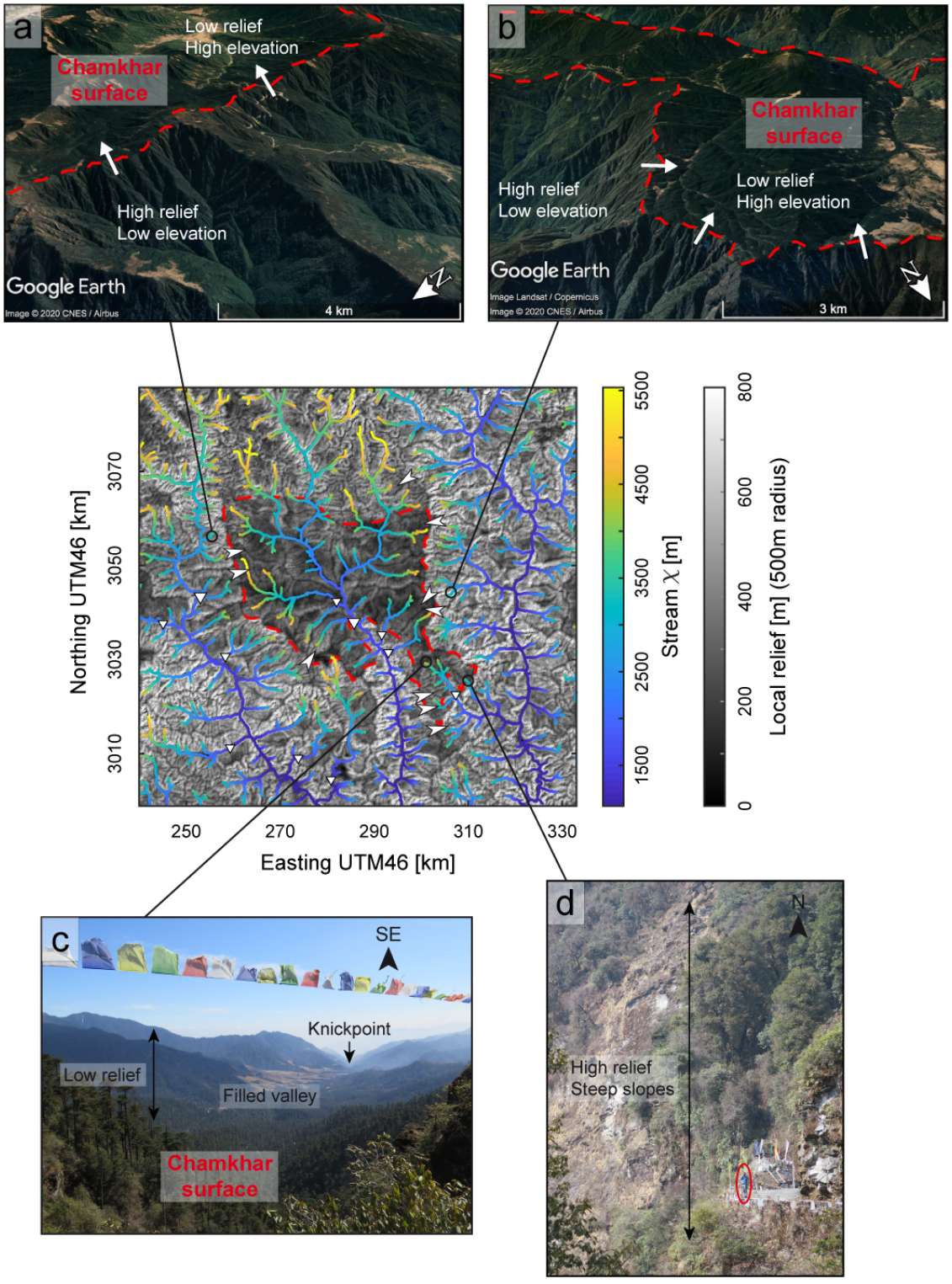
a
Low relief
High elevation
Chamkhar surface
High relief
Low elevation
Google Earth
Image © 2020 CNES / Airbus
4 km
N
b
Chamkhar surface
High relief
Low elevation
Low relief
High elevation
Google Earth
Image Landsat / Copernicus
Image © 2020 CNES / Airbus
3 km
N
Northing UTM46 [km]
3010
3030
3050
3070
250
270
290
310
330
Easting UTM46 [km]
Stream χ [m]
1500
2500
3500
4500
5500
Local relief [m] (500m radius)
0
200
400
600
800
c
SE
Knickpoint
Low relief
Filled valley
Chamkhar surface
d
N
High relief
Steep slopes

525

Figure 7 *(previous page)***: Divide mobility around the high-altitude low-relief Bumthang region, from χ metrics, field and satellite observations**. Central map (location on Figure 1c) represents local relief, with a moving window of 500 m, and the identified low-relief region is delimited by the red dashed line. Major knickpoints are reported with inversed triangles, and arrows locate the existence of morphological observations of regressive erosion (wind gaps), together with the direction of the associated divide migration. χ values are reported along the river network as a criterium to assess divide mobility (following (Willett et al., 2014)), and are determined for a concavity of 0.5. Other metrics for the mobility of the drainage divides around the Bumthang region are reported in Figure S3 (supplementary material). Similar observations are reported for the Wang surface (Figure S4 in supplementary material). Satellite observations are taken from the Google Earth database.

a) ©Google Earth view (Image from CNES - Airbus 2020) of the relief and elevation contrasts across the western drainage divide of the Bumthang surface. White arrows locate observed beheaded channels (wind gaps), and indicate the direction of deduced drainage divide migration.

b) ©Google Earth view (Image from CNES - Airbus 2020 and Landsat - Copernicus) of the relief and elevation contrasts across the eastern drainage divide of the Bumthang surface. White arrows locate observed beheaded channels, and indicate the direction of deduced drainage divide migration.

c) Field picture of the Sengor area (southeastern part of the Bumthang surface), where a filled valley is surrounded by higher relief rims. The filled valley is connected to the main river network by a tributary of the Kuri Chhu. A major knickpoint is present along this tributary, downstream of the pictured valley. Note the contrast in relief with picture d), across the local delimitation of the Bumthang surface.

d) Field picture illustrating the extremely steep hillslopes along the western Kuri Chhu valley, immediately east of the Bumthang surface. A person is standing on the lower right side of the picture for scale (red circle). Note the contrast in relief with picture c), across the local delimitation of the Bumthang surface.

4.4 Low-relief regions captured by secondary streams

At a more local spatial scale, modest high-altitude low-relief regions (Figures 3c-d) are connected to the main drainage network through secondary streams and tributaries, as for the Phobijka and Yarab regions (Figures 1c).

Starting from the profiles of Figure 6, we further explore the main features of the drainage network within and around the Phobijka surface using longitudinal and χ profiles of the secondary streams, with respect to their main trunk rivers, the Puna Tsang and Mangde Chhu (Figure 8). We here follow the approach proposed by (Yang et al., 2015) by differentiating streams draining the interior of this low-relief region and those flowing around. External streams (in green in Figure 8) have χ profiles mostly colinear with their main trunk stream - and more specifically with the local χ profile of their trunk stream, nearby their confluence. In contrast, streams draining the Phobijka low-relief surface (in red in Figure 8) plot well above the Puna Tsang or Mangde Chhu in χ coordinates, with a high and low steepness downstream and upstream of a major knickpoint, respectively.

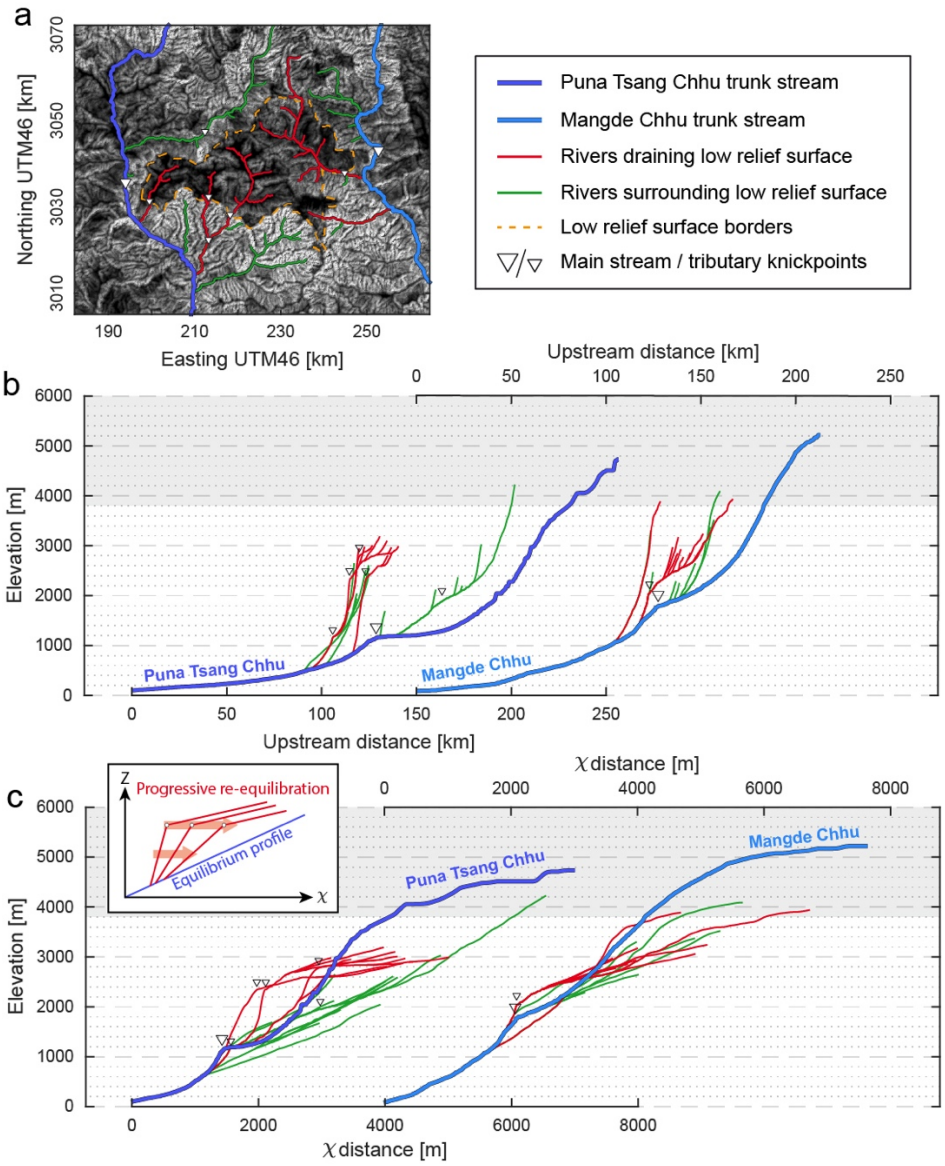

560

Figure 8: Longitudinal and transformed river profiles around and within the Phobijka high-altitude low-relief surface, following the approach of (Yang et al., 2015). Comparable results are verified for the Yarab surface (Figure S8 in supplementary material).

a) Map of topographic relief of the Phobijka area (see Figure 1c for location), with a moving window of 500 m (scale bar as in Figure 9); the identified low-relief region is delimited by the orange dashed line. Major knickpoints are reported with inversed triangles. Tributaries of

565 the Puna Tsang (west) and Mangde (east) Chhu trunk streams are color-coded, according to whether they drain the low-relief area (red) or are external to it (green).

b) Longitudinal river profiles of the Puna Tsang and Mangde Chhu, with main tributaries draining (red) or external (green) to the low-relief Phobijka area.

c) Transformed river profiles of the same rivers. Tributaries draining the low-relief area (red) plot above the main trunk streams as is observed in the case of area gain by river capture (Figure 4c). None of these profiles are concordant, indicating that these captures are not coeval and do not follow a coherent wave of incision propagating upstream. It should be noted that the higher the χ position of the knickpoints of the internal streams, the lower the steepness of the pirate streams downstream of their knickpoint. This is particularly illustrated by the Puna Tsang Chhu tributaries and is interpreted as reflecting progressive re-equilibration of pirate streams toward an equilibrium profile after capture (inset). Tributaries external to the low-relief area (green) are locally overall colinear with their main trunk stream, even though they gain drainage area by progressive divide migration (Figure 9).

Interestingly, the streams draining the Phobijka low-relief region have major knickpoints that are not concordant with the major knickpoint of their trunk stream in χ coordinates, with χ values and altitudes that vary by up to c.a. 1500 m and c.a. 1600 m, respectively, in the case of the Puna Tsang Chhu and its tributaries (Figure 8c). These streams show a peculiar pattern, most obvious in the case of the tributaries of the Puna Tsang Chhu : the greater the χ coordinate of the knickpoint, the lower the steepness of the stream segment downstream of the knickpoint, and therefore the closer (in χ coordinates) the stream profile gets to the regional average set by its trunk river (Figure 8c).

None of the streams have χ profiles clearly below the regional average driven by their main trunk channels (Figure 8c). It is also noteworthy that the χ profiles of the streams external to the Phobijka surface (in green in Figure 8) remain close to - and not above - the regional average imposed by their main trunk river (Figure 8), even though they keep gaining drainage area by regressive erosion of the low-relief area. Indeed, across-divide contrasts in χ, relief and elevation suggest that the Phobijka region is being regressively eroded all around by surrounding streams (Figure 9), in particular along its western divide with the Puna Tsang Chhu as contrasts in χ (Figure 9) and mostly elevation (Figure S6 in supplementary material) are highest. Contrary to the previous observations on low-relief regions drained by the Wang and Chamkhar Chhu (Figure 7, and Figures S3 and S4 in supplementary material), there is no evidence here for a counteracting drainage area expansion of the streams draining this low-relief region downstream of it (Figure 9). The area of this low-relief region is shrinking and the streams draining it are losing drainage area.

Similar observations are obtained for the streams draining inside and outside the Yarab low-relief region, located in eastern Bhutan and surrounded by the Kuri and Dangme Chhu (see Figures S7-S9 in supplementary material).

The characteristics of the streams draining elevated low-relief regions are interpreted as reflecting disequilibrium with drainage area gain by capture (Willett et al., 2014;Yang et al., 2015) (Figure 4c). Our results (Figures 8c, 9, and Figures S5-S9 in supplementary material) indicate that the discrete captures of low-relief regions has led to the punctual increase of drainage area of nearby pirate streams, but has not impeded the ongoing continuous regressive erosion of these regions - therefore accompanied by area loss - along their divide with other surrounding aggressor streams. Discordant knickpoints suggest that these captures were discrete and non-coeval, and that some of the pirate streams have had time to progressively partially re-equilibrate with their main trunk stream (inset in Figure 8c). In contrast, the streams aggressing all around elevated

low-relief regions are in overall equilibrium and keeping pace with the local incision set by their trunk streams, as indicated by their transformed profiles.

Figure 9 *(next page)***: Divide mobility around the high-altitude low-relief Phobijka region, from χ metrics, field and satellite observations**. Central map (location on Figure 1c) represents local relief, with a moving window of 500 m, and the identified low-relief region is delimited by the red dashed line. Major knickpoints are reported with inversed triangles, and arrows locate the existence of morphological observations of regressive erosion (wind gaps), together with the direction of the associated divide migration. χ values are reported along the river network, and are determined for a concavity of 0.5. Other complementary metrics of divide mobility are tested in Figure S6 (Supplementary material). Similar observations are reported for the Yarab region (Figure S7 in supplementary material). Satellite observations are taken from the Google Earth database.

a) Field picture illustrating the high relief and steep slopes along the Dang Chhu (tributary of the Puna Tsang Chhu), along the northern boundary of the Phobijka surface. Note the contrast in relief and slope with picture b), across the local delimitation of the Phobijka surface.

b) Field picture looking east of the Pele La pass (northern part of the Phobijka surface), where a filled valley is surrounded by higher relief rims. Note the contrast in relief with picture a), across the local delimitation of the Phobijka surface.

c) ©Google Earth view (Image from CNES - Airbus and Maxar Technologies 2020) of the relief and elevation contrasts across the northwestern drainage divide of the Phobijka surface. White arrows locate observed beheaded channels (wind gaps), and indicate the direction of deduced drainage divide migration.

d) ©Google Earth view (Image from CNES - Airbus 2020) of the relief and elevation contrasts across the southern limit of the Phobijka surface. White arrows locate observed beheaded channels, and indicate the direction of deduced drainage divide migration.

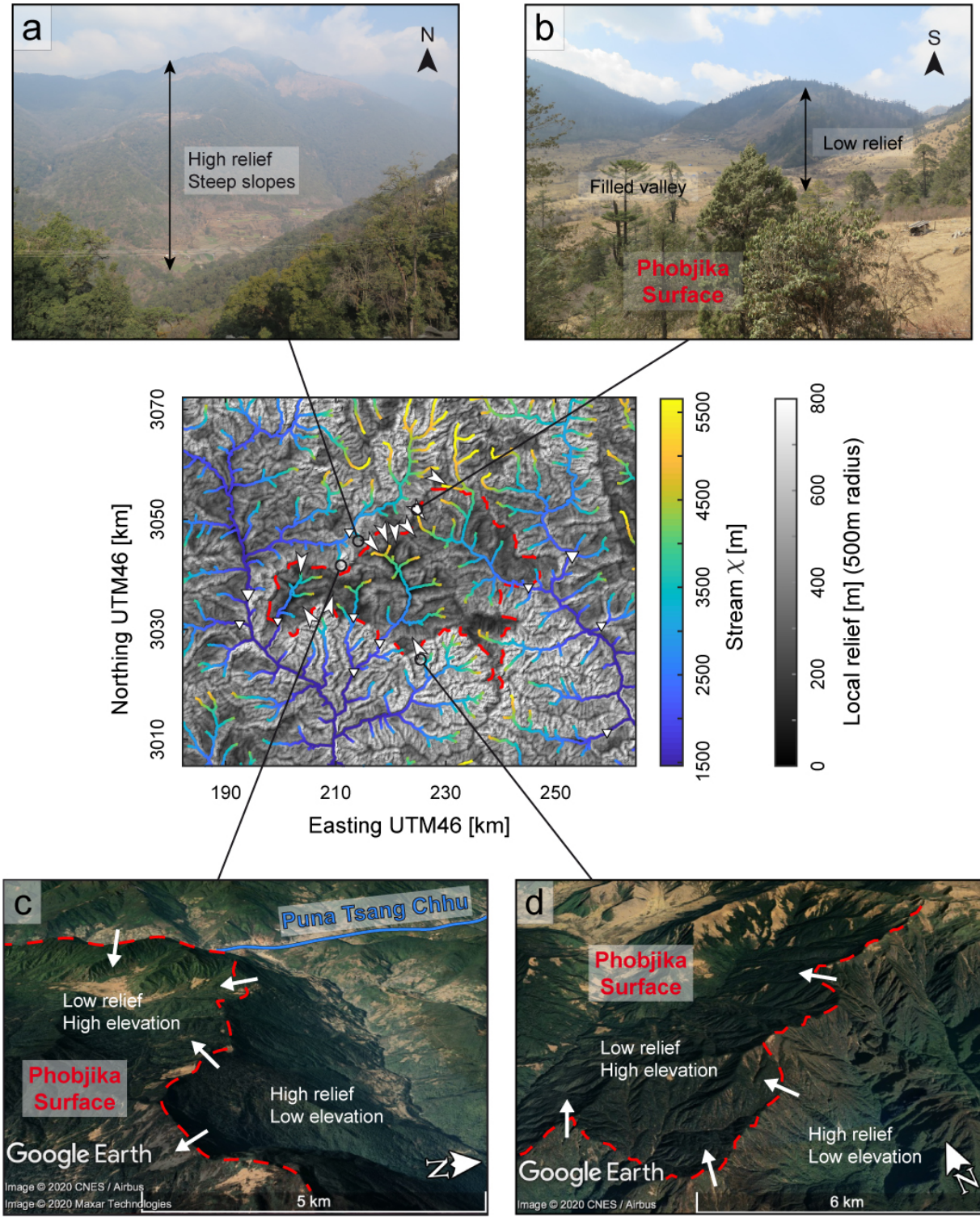
a
N
High relief
Steep slopes
b
S
Low relief
Filled valley
Phobjika
Surface
Northing UTM46 [km]
3070
3050
3030
3010
190
210
230
250
Easting UTM46 [km]
Stream χ [m]
5500
4500
3500
2500
1500
Local relief [m] (500m radius)
800
600
400
200
0
c
Puna Tsang Chhu
Low relief
High elevation
Phobjika
Surface
High relief
Low elevation
Google Earth
Image © 2020 CNES / Airbus
Image © 2020 Maxar Technologies
5 km
d
Phobjika
Surface
Low relief
High elevation
High relief
Low elevation
Google Earth
Image © 2020 CNES / Airbus
6 km

630

4.5 Summary of key results

Altogether, we do not find in our results and field observations any evidence that the morphological characteristics of Bhutan were generated by a common wave of incision propagating upstream the drainage network. Indeed, all river profiles and their knickpoints are discordant in χ transformed coordinates (Figures 5c, 6b and 8c - by comparison to Figure 4b), whatever the spatial scale of investigation. This finding is supported by the secondary drainage network of rivers flowing through or around high-altitude low-relief regions since all these streams share a common base level and their χ profiles can be more rigorously compared (Figure 8c). The documented χ profiles of major or secondary rivers support the existence of ubiquitous discrete and non-coeval river captures of low-relief regions in Bhutan.

Our results also suggest that a steady state morphology is far from being reached in the Bhutan Himalaya. Only few major rivers (the Kuri and Dangme Chhu, and to some extent the Puna Tsang and Mangde Chhu) have profiles associated with a potential equilibrium with tectonic and climatic forcing throughout the mountain range. The other large Himalayan rivers (Chamkhar and Wang Chhu) keep a record of large-scale captures, and show peculiar dynamics on either side of their major knickpoint, with apparent drainage area loss and expansion upstream and downstream of the knickpoint, respectively (Figure 7). This dynamic response of rivers is more pronounced at smaller spatial scales, where some secondary streams have captured high-altitude low-relief regions, and where others are progressively gaining drainage area by the regressive erosion of these same regions (Figures 8-9).

5 Discussion

5.1 Limits on our analysis and results

5.1.1 Limits related to possible lateral variations in tectonics or climate.

The comparison between the various Himalayan rivers throughout Bhutan may be limited by possible lateral variations in boundary and forcing conditions. The widespread occurrence of Greater Himalayan series (Figure 1a) limits large-scale lithological variations. Tethyan or Lesser Himalayan series are also present in Central and Eastern Bhutan. However, spatial variations in bedrock erodibility associated with these variations is expected to be limited (Lavé and Avouac, 2001;Adams et al., 2020).

Climate is everywhere tropical and wet. Precipitation varies mostly along a latitudinal transect across the range, with extreme precipitation rates of over 6 m/yr along the mountain front (Baillie and Norbu, 2004;Bookhagen and Burbank, 2006;Grujic et al., 2006). Within our region of interest in the mountain hinterland, present-day precipitation rates are everywhere relatively moderate, with values of c.a. 1-2 m/yr. Longitudinal variations from east to west related to the

rainshadow formed by the Shillong Plateau in the foreland are minor. As large rivers are mostly flowing north-south, perpendicular to the main climatic trend, they are all similarly affected and the cross-comparison of river profiles as done here is permitted.

The Amo and Wang Chhu are the two rivers of westernmost Bhutan where significant lateral structural and tectonic variations may be expected, as they are located in the vicinity of the Paro structural window and of the Yadong graben (e.g. (Gansser, 1983;Long et al., 2011a;Greenwood et al., 2016)) (Figure 1a). Similarly, a structural window into Lesser Himalayan series prevails along the Kuri Chhu (Figure 1a), where variations in the seismic coupling of the MHT have been recently evidenced (Marechal et al., 2016), suggesting other possible lateral variations in tectonics further east. In Western and Eastern Bhutan, we therefore cannot exclude the possibility of a tectonic forcing different from that encountered in Central Bhutan.

It should be noticed that the profiles and characteristics of the Wang and Amo Chhu in Western Bhutan are overall comparable to those of the Chamkhar Chhu in Central Bhutan. Additionally, the Yarab high-altitude low-relief surface in Eastern Bhutan shares common attributes with the Phobijka low-relief patch in Central West Bhutan. In general, most geomorphic features specific to the Bhutan Himalayas are found along a longitudinal band throughout this whole region of the Himalayas (Figure 1c). Together these observations suggest that the lateral variations in tectonics, climate or lithology documented in Bhutan may have only a minor effect on the observed morphology.

5.1.2 Limits related to the morphometric approach.

The comparison of river profiles in χ transformed coordinates requires a common base level for all streams. Tributaries with a common trunk stream meet this specific condition, but the comparison of major rivers with different and independent outlets is not straightforward. To overcome this limitation, we assume that the base level of all major rivers is the Gangetic Plain, which has an almost constant elevation of c.a. 100-120 m south of the mountain front. For this reason, the absence of evidence for a coherent wave of incision is mostly evidenced from the joint analysis of tributaries and of their trunk stream (Figure 8c), and only suggested by the comparison of major rivers (Figure 5b).

A coherent wave of incision migrating upstream the drainage network may not be straightforward to elucidate in transformed χ profiles in the case of an unstable drainage network, where divide migration and captures prevail throughout the landscape. This has been illustrated in field cases where the dispersion of knickpoints (in transformed coordinates) associated to the upstream migration of a wave of incision is interpreted to relate to the coeval changes in upstream drainage area due to divide migration (Schwanghart and Scherler, 2020) or river captures (Giachetta and Willett, 2018). In the case of the Bhutan Himalaya, river captures leave a clear and significant imprint on the river network (Figures 5b and 8c) and may hide the signature of other processes. As further discussed hereafter (see section 5.2), the river network appears to adjust much faster to progressive changes in drainage area due to the mobility of divides, so that the affected streams keep adjusting to the incisional pace of their trunk river or to changes of main river base level. This results in the fact that divide migration does not leave a specific signature on the transformed profiles of these rivers (Figure 8c), which would have permitted here for keeping the record of an incision wave if existent.

χ analyses are based on the stream power concept and do not include the effect of sediments on river incision (Gasparini et al., 2007). This can limit our interpretations for rivers with alluvial plains or for secondary streams capturing low-relief regions. It has been shown that discordant χ profiles could be achieved for rivers enduring a common wave of incision when incision is dependent on the sediment flux (Giachetta and Willett, 2018). In this case, a positive correlation between drainage area and upstream knickpoint migration is expected as drainage area supposedly approximates available sediment fluxes (Giachetta and Willett, 2018), which we have not clearly found in our data (Figure S8 in supplementary material).

When calculating χ values and transformed river profiles, drainage area is taken as a proxy for river discharge (equation 1) (e.g.(Perron and Royden, 2013)). This implies that precipitation rates are supposedly constant over the considered drainage basin, an assumption not verified here (Bookhagen and Burbank, 2006;Grujic et al., 2006) as in most large-scale watersheds. Spatial variations in rainfall have been shown to alter river profiles (Han et al., 2014;Han et al., 2015). Here, locally higher than average precipitation rates lead to locally higher river discharges, and may be mistaken for a false gain in drainage area. This should not, however, alter and impact our results and interpretations. First, extreme precipitation rates are only found along the mountain front in Bhutan, by c.a. 50 km north of physiographic transition T1 at most, and therefore south of our region of interest where major knickpoints (Figure 5a) and high-altitude low-relief regions (Figures 2ab) are found. Last, our interpretations rely on the cross-comparison of river profiles that are all expected to be similarly affected as all large rivers flow across the main north-south climatic trend.

Some of our inferences are therefore dependent on the known limitations of χ analyses and of the stream power approach in general. However, these should not affect our main conclusions on river captures or migrating divides - and therefore on the unstable and dynamic pattern of the river network -, as they are based on the cross-comparison of rivers affected by overall similar latitudinal tectonic and climatic forcing, and are further corroborated by field and satellite observations, as well as by across-divide contrasts in Gilbert metrics (Figures 7 and 9, and Figure S3-S4 and S6-S7 in supplementary material).

5.2 River captures, migrating divides and time scales of landscape response

Secondary streams external to low-relief areas progressively gain drainage area by regressive erosion (Figures 7 and 9). Transformed profiles of these tributaries remain close to the regional trend of trunk channels (Figure 8c). This observation suggests that the channel response is here faster than that of the perturbation driven by divide migration, consistent with conclusions from recent numerical experiments by (Whipple et al., 2017b). This result implies that drainage re-organization by progressive divide migration is not expected to leave a particular geomorphic signature, most probably because of a relatively high erosional efficiency (Whipple et al., 2017b), in contrast with other field cases where the time for divide migration may have outpaced that of the erosional river response (Schwanghart and Scherler, 2020).

Only drainage area increase by discrete stream capture appears to leave a significant imprint on the river network. Our results suggest that river captures have occurred at all spatial scales in the hinterland of Bhutan, from large-scale captures in the case of the Wang or Chamkhar Chhu, with high (> 1 km) major knickpoints (Figure 5b), to more modest captures in the case of the secondary streams draining high-altitude low-relief regions (Figure 8). Discordant profiles and the observed variable position of knickpoints in χ coordinates and altitude favor the idea that these captures are discrete and not coeval in time, and that pirate streams have been progressively returning to equilibrium (Figure 8c). These captures result in a large and abrupt drainage area increase, which requires a subsequent longer time for the rivers to adapt to their new boundary conditions. Such particular conditions are discussed by (Whipple et al., 2017b) using the relative ratio of the time scale of channel response to a characteristic recurrence time of large capture events. Following this reasoning, our results suggest that river captures leave an imprint on river profiles if captures occur more often than the time needed to adjust to their new conditions, or if the last capture event is younger than the time scale for channel response. These various considerations imply that only the most recent landscape evolution can be retrieved from morphometric approaches, leaving little - if no - possibility to access the morphologic conditions prior to the most recent captures.

5.3 Geomorphological characteristics of the Bhutan Himalaya

Our results were previously presented following the various spatial scales of investigation. Below, we provide a synthesis of our observations for each geomorphic feature whatever associated spatial scale, and discuss possible explanations of their origin. We finally compare our findings and inferences to previous interpretations.

5.3.1 Major knickpoints within the river network

Knickpoints along large Himalayan rivers of Bhutan separate two domains, with drainage area expansion downstream of the knickpoint and drainage area reduction upstream (Figure 7, and Figures S3-S4). Such dynamics on either side of a knickpoint have already been observed in other contexts of major river captures, such as for the Duero river in Spain and Portugal (Struth et al., 2019). The tool effect of sediments remobilized from the upstream captured alluvial plain may favor incision downstream of the knickpoint, that would propagate laterally towards the divides and lead locally to the outward expansion of drainage area. Such consequent drainage area gain may additionally boost river incision and the lowering of the local base level. These positive feedbacks are expected to favor and enhance the upstream migration of the major knickpoint (e.g. (Giachetta and Willett, 2018;Struth et al., 2019)). However, an additional - but negative - feedback may operate as the drainage area reduction upstream of the knickpoint may limit and refrain the upstream knickpoint migration (Schwanghart and Scherler, 2020). Such feedback, by eventually significantly lowering the expected upstream migration of major knickpoints, may contribute to the preservation and surface uplift of the upstream low-relief region over time, to the over-steepening of the downstream river segments and therefore to the large dimensions of observed major knickpoints. If the reduction in the rate of knickpoint migration by upstream drainage area loss were significant, knickpoints along major Bhutanese rivers could appear as more or less stationary.

Major knickpoints are observed at all scales (Figure 6). They follow a specific spatial organization as most of them are localized in the Bhutan hinterland, nearby physiographic transition T2, regardless of the size of the associated drainage basin (Figures 1b-c and 5a). This co-location looks surprising in the case of non-coeval discrete stream captures at various spatial scales. It may therefore suggest that knickpoint migration remains limited in space, nearby T2. This indicates that these knickpoints originated and have possibly been maintained locally.

5.3.2 High-altitude low-relief regions

Transformed profiles of the rivers draining elevated low-relief regions all show a specific pattern indicative of river captures, regardless of their spatial scale (Figures 5b and 8c). Discordant χ profiles at all scales (Figures 5b, 6b and 8c) suggest that these captures were not coeval. Conversely, no evidence for a counteracting drainage area loss by stream piracy appears in χ profiles of nearby rivers, as none of the profiles are below the regional equilibrium line delineated by the profiles of large Himalayan rivers (Figure 5b) or of trunk streams in the case of secondary low-relief regions (Figure 8c). It has been noticed that area loss by piracy is not as well expressed in transformed coordinates as is area gain by capture (see Figure 9b of (Whipple et al., 2017b)). Because the absence of χ river profiles below estimated regional averages is observable at all spatial scales, even when large-scale captures are suspected, it could be postulated that such captures have not been at the expense of other rivers, but of the low-relief regions themselves if once isolated from the drainage network. Even though not common, internally drained basins exist in tropical contexts. The Sun Moon Lake region of Central Taiwan is an example, where internally drained basins are on the verge of being captured (Toushe Basin), or where similar captures are suspected (Yushi and Puli Basins) (see discussion by (Simoes et al., 2014)). Because the time scale for river response to changes in boundary conditions is expected to be relatively short in Bhutan (see section 5.2), the conditions that lead to the relief lowering and isolation of the landscape patches investigated here, prior to their capture, may not have left a clear morphologic record.

Swath profiles across the Bhutan hinterland illustrate that elevated low-relief regions have overall similar altitudes and local relief (Figure 10), regardless of their spatial scale, as if resulting from the surface uplift and subsequent dissection of the same initial topographic surface (after (Whipple et al., 2017a)). However, morphometric analyses may mostly detect the lowest-relief patches, as these offer the highest relief contrast with other regions (Figure 1c). We cannot therefore discard the possibility that other low-relief patches (but with relatively higher relief) exist at other altitudes, as suspected for instance to the east and north-east of the Yarab region (Figure S8 in supplementary material). In the case that relief reduction is concomitant to surface uplift, such as when low-relief regions are formed by area loss during drainage re-organization (Whipple et al., 2017a), local relief is expected to correlate with altitude. The similar altitude and local relief of low-relief regions (Figure 10) may therefore either favor the idea of local remnants of relict landscapes or be indicative of the in-situ formation of these regions during uplift.

The limits of these regions most often coincide with drainage divides ("coincident divides" in the sense of (Willett, 2017)) with numerous beheaded channels, in particular for secondary regions (Figures 7 and 9). This observation, together with that of local low denudation rates (Adams et al., 2016) and relief (Figures 7 and 9), of alluvial filling (Figures 3d-e) and

well-developed soils (Figures 3b-d) (Baillie et al., 2004;Adams et al., 2016) in valleys surrounded by higher-relief rims (Figures 3b, 3d, 7 and 9), favors the idea that these low-relief regions were formed in-situ while uplifted, before their capture (Willett, 2017). Area loss related to the dynamic re-organization of the drainage network (after (Willett et al., 2014;Yang et al., 2015)) could be a plausible mechanism given the ample evidence for captures and divide mobility. A local rise in base level, as in the case of defeated uplifted hanging valleys is another possibility, as described in other contexts (e.g. (Burbank et al., 1996;Fernandez-Blanco et al., 2020)).

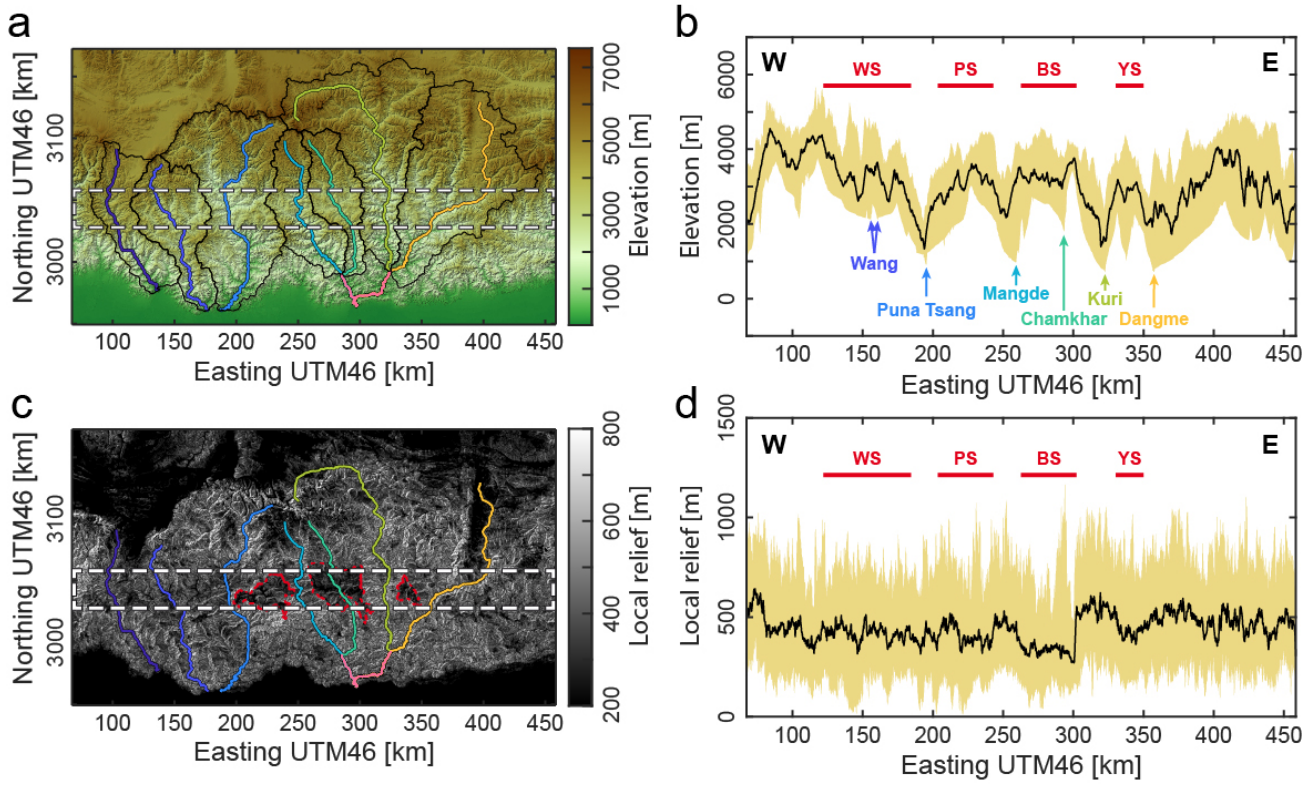

Figure 10: Topography and relief along the hinterland of the Bhutan Himalaya, where low-relief surfaces are located.

WS: Wang Surface; PS: Phobijka Surface; BS: Bumthang Surface; YS: Yarab surface.

a) Topographic map of the Bhutan Himalaya from ALOS World 3D – 30m (AW3D30) DEM data. Main drainage basins are delineated by black lines and associated main rivers are color-coded (color-code as in Figure 1). The dashed rectangle locates the swath profile represented in b).

b) Topographic swath profile along the Bhutan hinterland, with elevations taken within the band illustrated in Figure 10a. Location of major rivers and of low-relief regions are reported.

c) Map of local relief, as calculated from the topography shown in Figure 10a, with a moving window of 500 m. Major high-altitude low relief areas are delineated by dashed red lines. Main rivers are located and color-coded. The dashed rectangle locates the swath profile represented in d) and encompasses the same region as that of Figure 10a.

d) Swath profile of relief along the Bhutan hinterland, with relief taken within the band located in Figure 10c. Low-relief regions of the mountain range interior are reported. The lower relief values of the swath profile are to be considered for low-relief regions.

These possible interpretations only describe the type of morphological response of the river network leading to the formation of these features (relief lowering and isolation of these regions), but do not provide the processes driving this response. We emphasize that the high-altitude low-relief regions are all co-located in the hinterland of Bhutan, in between physiographic transitions T2 and T3, whatever their spatial scales and dimensions (Figure 1c). This strongly suggests that they were most probably formed only locally and not pervasively throughout Bhutan, appealing for a local process driving and supporting their formation, preservation and subsequent dissection.

5.3.3 The spatial organization of all major knickpoints and low-relief regions calls for a common local tectonic origin

Our investigations illustrate the highly dynamic - and eventually unstable - pattern of the river network in the Bhutan hinterland. Despite these dynamics, both major knickpoints and high-altitude low-relief regions, whatever their spatial scale, all co-locate in the hinterland of the Bhutan Himalaya, along an approximately west-east oriented spatial band nearby physiographic transition T2 or in between T2 and T3 (Figures 1b-c). This observation calls for a common local genetic origin for all these features and for the observed network dynamics. This holds throughout most of the Himalayas of Bhutan, even in Eastern Bhutan where no major knickpoint exists along the Kuri and Dangme Chhu at these latitudes (Figures 1 and 5). The presence of the Yarab low-relief region, localized in between these two major rivers (Figures 1c), indicates that a similar mechanism is also ongoing in this part of the Himalayan range (Figures S7-S9 in supplementary material). The absence of a major knickpoint on adjacent large rivers reveals that these have sufficient power to adjust to local conditions. The only minor exception to the observed colocation is the major knickpoint of the Wang Chhu in Western Bhutan, which is deported c.a. 20-30 km southward from the observed longitudinal band (Figures 1 and 5a).

This spatial geomorphological organization is not expected to be controlled lithologically as it is clearly not correlated to surface geology (Figure 1a). Alternatively, the orientation of the swath containing all major knickpoints and low-relief regions supports the idea of a local tectonic driver in the mountain hinterland, as this orientation is parallel to major active tectonic structures (such as the frontal MFT or MBT - Figure 1a) or associated geomorphic expressions (such as the High Himalayan range expectedly above a mid-crustal ramp of the MHT) (Figure 1b and 2).

Additionally, the east-west swath encompassing the investigated geomorphic peculiarities of the Bhutan Himalaya also approximately follows the orientation of the precipitation pattern in Bhutan, and is slightly north of the band of highest precipitation rates (e.g. (Bookhagen and Burbank, 2006;Grujic et al., 2006)). Such climatic pattern results from the major

orographic barrier formed by the steeply rising topography between physiographic transitions T1 and T2 (Figures 2a-b), for which tectonics is the most probable driver. As such, we propose that the peculiar geomorphic dynamics, the steep topography between T1 and T2 and the associated local climatic pattern all share an initial common tectonic driver. The observed and investigated landscape characteristics is therefore interpreted to first reflect active tectonics in the hinterland of Bhutan, but the interplay between local uplift, the associated high slopes and climate may modulate and enhance local landscape dynamics (e.g. (Adams et al., 2020)).

5.3.4 Discussing previous interpretations in light of our findings

The absence of evidence for a coherent wave of incision moving upstream the drainage network (Figures 5b, 6b and 8c) and the spatial organization of observed geomorphic features only along a longitudinal band (Figure 1), exclude previous interpretations relying on any large-scale change in tectonics or climate over Bhutan. This is the case for the model of tectonic rejuvenation of Bhutan relative to the Himalaya of Central Nepal (Duncan et al., 2003), or for that of a general surface uplift of Bhutan consequent to decreasing precipitations in the rainshadow of the rising Shillong Plateau (Grujic et al., 2006). The dimensions of the major knickpoints of some of the large rivers, with heights of > 1km in the cases of the Amo, Wang or Chamkhar Chhu (Figures 2c and 5), are most probably too large to be related to a wave of incision migrating upstream into a relict landscape, as a response to a change in relative base level.

(Baillie and Norbu, 2004) proposed that the variety of river profiles were related to lateral variations in tectonic uplift throughout Bhutan. This may potentially explain part of the discordance in χ profiles of major and large rivers (Figure 5b). In this case the spatial co-location of knickpoints throughout Bhutan, within a west-east swath (Figures 1 and 5a), would indicate that the location of active tectonics is coherent along strike but that only the rates of active deformation are laterally variable. Even though lateral variations in the rates of uplift cannot be excluded, these are not expected to vary significantly, and in particular randomly from one valley to the other. Additionally, the similar steepness of large rivers south of T2, located variably in western (Puna Tsang Chhu), central (Mangde Chhu) and eastern (Kuri and Dangme Chhu) Bhutan (Figure 5b) calls for overall similar rates of uplift, given the similar lithologic (Figure 1a) and climatic (e.g. (Bookhagen and Burbank, 2006;Grujic et al., 2006)) conditions. This interpretation is supported by the fact that the theoretical steepnesses of the proto- Wang and -Chamkhar Chhu, prior to their suspected large-scale captures, are similar to that of these other large rivers, south of T2 (Figure 5c). Also, the presence of the high-altitude low-relief Yarab surface in eastern Bhutan indicates that similar first-order conditions prevail in this part of the Himalaya even though the two major surrounding rivers (the Kuri and Dangme Chhu) have no major knickpoint. Similar tectonics, in terms of patterns and also in terms of rates, are therefore expected throughout Bhutan despite the variability of fluvial profiles. In fact, this variability is rather expected to relate to the various responses and capacities of the different rivers to adjust to local tectonics (Figure S10 in supplementary material), and to the existence or not of recent captures.

(Adams et al., 2016) proposed that major knickpoints and low-relief regions were the geomorphic response to recent uplift over a blind duplex in the Bhutan hinterland. Interestingly coming at it from another angle, their interpretation meets our

deductions that the observed geomorphic features need to be primarily sustained locally by ongoing active uplift. The proposed tectonic perturbation originates in the hinterland and not at the base level of major rivers, which may account to some extent for discordant χ profiles (Figure 5b). Our results therefore confirm their primary conclusion on the need for active tectonics in the hinterland, and additionally document some aspects of the landscape dynamics that were not explored.

To move a step forward, some details of the (Adams et al., 2016) model could be refined in light of our findings. Major knickpoints were interpreted by these authors as setting the local base level for the in-situ filling of upstream uplifted valleys. In their model, knickpoints migrate upstream and upwards, and while doing so remove fill deposits. If this were the case, upstream knickpoint migration (from the tectonic perturbation) would be expected to correlate with knickpoint altitude, upstream drainage area and the extent of uplifted alluvial fill, which is not specifically observed (Figure S10 in supplementary material). Indeed, the co-location of all major knickpoints whatever considered spatial scale, from major to local rivers (Figure 1), indicates that these knickpoints are relatively stationary (see section 5.3.1). Our deductions meet (Adams et al., 2016)'s conclusions that high-altitude low-relief regions were formed in-situ while uplifted. We find, however, evidence that these regions may have been defeated and isolated once from the main network before being captured (see section 5.3.2), which contrasts with the continuously through-flowing and adjusting uplifted rivers supported by (Adams et al., 2016). Such differences in the details of the origin and evolution of the low-relief regions become important when it comes to derive surface uplift from a theoretical (poorly resolved) initial river profile by comparison to the present-day profiles. One possible future research direction aiming at better understanding the dynamics of major knickpoints and the formation and evolution of low-relief regions in Bhutan would be to model the landscape evolution in response to local uplift in the mountain hinterland, following the initial work of (Adams et al., 2016) but adding the dynamic response of the river network through migrating divides and river captures. Finally, denudation rates should be considered with great caution when used as proxys for uplift rates in places where the shape of drainage basins is far from being stable, as is the case here (e.g. (Sassolas-Serrayet et al., 2019)). It should be also emphasized that uplift rates are expected to vary across strike, with higher rates over the blind ramp and with lower rates downstream and upstream of it, further challenging the comparison between denudation rates measured in high-relief canyons and those in upstream alluvial or isolated low-relief valleys.

6 Conclusion

Based on field observations and on a quantitative and qualitative morphometric analysis of the mountain hinterland in Bhutan at various spatial scales, we have further documented the landscape dynamics of this part of the Himalayas where out-of-equilibrium morphologies have been described. We find that the various geomorphic features of the Bhutanese landscape, such as major knickpoints or high-altitude low-relief regions, are most probably not related to the migration of a wave of incision upstream the river network. Rather, our analysis emphasizes the existence of numerous drainage captures, at various spatial scales, spatially discrete and temporally non-coeval, with partial re-equilibrations of captured drainages in some

cases. In addition to these captures, drainage divides are found to migrate in various parts of the hinterland, in particular around or downstream elevated low-relief regions, with efficient re-equilibration of river profiles as expected in the case of relatively fast landscape response.

Our results therefore emphasize the existence of an unstable and dynamic landscape, which however obeys a specific spatial organization along a longitudinal spatial band in the mountain range interior. This latter key observation supports the idea that the documented geomorphic dynamics needs to be sustained locally by tectonic uplift. Even though the idea proposed by (Adams et al., 2016) of uplift over a blind ramp in the hinterland is consistent with our conclusions, some of their deductions do not capture or account for the observed high dynamics of the river network. This is most probably because they base their deductions on the comparison to a landscape evolution simulation in which drainage divides remain stationary. Future work exploring the initial idea of (Adams et al., 2016) of active tectonic uplift in the mountain hinterland but with account on the possible dynamic response of the river network is therefore needed.

Finally, because the drainage network is not stable with ubiquitous divide migrations in the hinterland, the previous use of denudation rates as a proxy for tectonic uplift rates in Bhutan (Le Roux-Mallouf et al., 2015;Adams et al., 2016) may be problematic, and results should be re-evaluated. Our work, therefore emphasizes the need for a precise investigation of landscape dynamics and disequilibrium over various spatial scales as a first essential step in morpho-tectonic studies of active landscapes.

Supplement material

Additional figures are provided as supplementary material.

Author Contribution

MS designed and conceptualized the research objectives of this study. She also wrote the main draft of the manuscript with contributions from all co-authors. TSS carried the presented geomorphic analyses and prepared all associated figures. RC gathered all the necessary financial support that led to the work presented here. All co-authors participated to field work, scientific discussions and the co-editing of the manuscript.

Competing interests

The authors declare that they have no conflict of interest

Acknowledgements

This manuscript benefitted from constructive comments by W. Schwanghart and an anonymous reviewer, and Associated Editor S. Castelltort is thanked for the handling of the manuscript. The fruitful discussions that led to this manuscript rose during field work in Bhutan, and our friend and driver Phajo Kinley (Department of Geology and Mines, Thimphu) is warmly

thanked for taking good care of us all during our various journeys. Through the work of MS, this study stands as IPGP contribution # 4223.

Financial support

This study benefitted from grants from the Agence National de la Recherche (France) attributed to RC, through projects ANR BhutaNepal (ANR grant # ANR-13-BS06-0006) and TopoExtreme (ANR grant # ANR-18-CE01-0017). TSS benefitted from a PhD grant attributed by the French Ministry of Higher Education and Research. Through the work of MS, this study contributes to the IdEx Université de Paris ANR-18-IDEX-0001.

References

Adams, B. A., Hodges, K. V., van Soest, M. C. and Whipple, K. X.: Evidence for Pliocene-Quaternary normal faulting in the hinterland of the Bhutan Himalaya., Lithosphere, 5, 438-449, 2013.

Adams, B. A., Hodges, K. V., Whipple, K. X., Ehlers, T. A., van Soest, M. C. and Wartho, J.-A.: Constraints on the tectonic and landscape evolution of the Bhutan Himalaya from thermochronometry., Tectonics, 34, 1329-1347,https://doi.org/10.1002/2015TC003853, 2015.

Adams, B. A., Whipple, K. X., Forte, A. M., Heimsath, A. M. and Hodges, K. V.: Climate controls on erosion in tectonically active landscapes., Science Advances, 6,https://doi.org/10.1126/sciadv.aaz3166, 2020.

Adams, B. A., Whipple, K. X., Hodges, K. V. and Heimsath, A. M.: In situ development of high-elevation, low-relief landscapes via duplex deformation in the Eastern Himalayan hinterland, Bhutan, Journal of Geophysical Research, 121, 294-319,https://doi.org/10.1002/2015JF003508, 2016.

Adlakha, V., Lang, K. A., Patel, R. C., Lal, N. and Huntington, K. W.: Rapid long-term erosion in the rain shadow of the Shillong Plateau, Eastern Himalaya., Tectonophysics, 582, 76-83,https://doi.org/10.1016/j.tecto.2012.09.022, 2013.

Allen, P. A.: From landscapes into geological history, Nature, 451, 274-276,https://doi.org/10.1038/nature06586, 2008.

Babault, J., Bonnet, S., Van Den Driessche, J. and Crave, A.: High elevation of low-relief surfaces in mountain belts: does it equate to post-orogenic surface uplift?, Terra Nova, 19, 272-277,https://doi.org/10.1111/j.1365-3121.2007.00746.x, 2007.

Babault, J., Van Den Driessche, J. and Teixell, A.: Longitudinal to transverse drainage network evolution in the High Atlas (Morocco): The role of tectonics., Tectonics, 31,https://doi.org/10.1029/2011TC003015, 2012.

Baillie, I. C. and Norbu, C.: Climate and other factors in the development of river and interfluve profiles in Bhutan, Eastern Himalayas, Journal of Asian Earth Sciences, 22, 539-553, 2004.

Baillie, I. C., Tshering, K., Dorji, T., Tamang, H. B., Dorji, T., Norbu, C., Hutcheon, A. A. and Baumler, R.: Regolith and soils in Bhutan, Eastern Himalayas., European Journal of Soil Science, 55, 9-27,https://doi.org/10.1046/j.1365-2389.2003.00579.x, 2004.

Beaumont, C., Jamieson, R. A., Nguyen, M. H. and Lee, B.: Himalayan tectonics explained by extrusion of a low-viscosity crustal channel coupled to focused surface denudation, Nature, 414, 738-742,https://doi.org/10.1038/414738a, 2001.

Beeson, H. W., McCoy, S. W. and Keen-Zebert, A.: Geometric disequilibrium of river basins produces long-lived transient landscapes, Earth and Planerary Science Letters, 475, 34-43,https://doi.org/10.1016/j.epsl.2017.07.010, 2017.

Berthet, T., Ritz, J.-F., Ferry, M., Pelgay, P., Cattin, R., Drukpa, D., Braucher, R. and Hetenyi, G.: Active tectonic of the eastern Himalaya: new constraints from the first tectonic geomorphology study in southern Bhutan., Geology, 42, 427-430, 2014.

Bilham, R.: Himalayan earthquakes: a review of historical seismicity and early 21st century slip potential., Geological Society, London, Special Publications, 483,https://doi.org/10.1144/SP483.16, 2019.

Biswas, S., Coutand, I., Grujic, D., Hager, C., Stockli, D. and Grasemann, B.: Exhumation and uplift of the Shillong Plateau and its influence on the eastern Himalayas: New constraints from apatite and zircon (U-Th-[Sm])/He and apatite fission track analyses., Tectonics, 26,https://doi.org/10.1029/2007TC002125, 2007.

Bollinger, L., Avouac, J. P., Beyssac, O., Catlos, E. J., Harrison, T. M., Grove, M., Goffé, B. and Sapkota, S.: Thermal structure and exhumation history of the Lesser Himalaya in central Nepal, Tectonics, 23, TC5015,https://doi.org/10.1029/2003TC001564, 2004.

Bollinger, L., Henry, P. and Avouac, J. P.: Mountain building in the Nepal Himalaya: Thermal and kinematic model., Earth and Planerary Science Letters, 244, 58-71,https://doi.org/10.1016/j.epsl.2006.01.045, 2006.

Bonnet, S. and Crave, A.: Landscape response to climate change: Insights from experimental modeling and implications for tectonic versus climatic uplift of topography., Geology, 31, 123-126, 2003.

Bookhagen, B. and Burbank, D. W.: Topography, relief, and TRMM-derived rainfall variations along the Himalaya., Geophysical Research Letters, 33,https://doi.org/10.1029/2006GL026037, 2006.

Burbank, D. W., Blythe, A. E., Putkonen, J., Pratt-Sitaula, B., Gabet, E., Oskin, M., Barros, A. and Ojha, T. P.: Decoupling of erosion and precipitation in the Himalayas, Nature, 426, 652-655,https://doi.org/10.1038/nature02187, 2003.

Burbank, D. W., Meigs, A. and Brozovic, N.: Interactions of growing folds and coeval depositional systems., Basin Research, 8, 199-223,https://doi.org/10.1046/j.1365-2117.1996.00181.x, 1996.

Castelltort, S., Goren, L., Willett, S. D., Champagnac, J.-D., Herman, F. and Braun, J.: River drainage patterns in the New Zealand Alps primarily controlled by plate tectonic strain, Nature Geoscience,https://doi.org/10.1038/NGEO1582, 2012.

Cattin, R. and Avouac, J. P.: Modeling mountain building and the seismic cycle in the Himalaya of Nepal, Journal of Geophysical Research, 105, 13389-13407, 2000.

Clark, M. K. and Bilham, R.: Miocene rise of the Shillong Plateau and the beginning of the end for the Eastern Himalaya., Earth and Planerary Science Letters, 269, 337-351,https://doi.org/10.1016/j.epsl.2008.01.045., 2008.

Clift, P. D., Giosan, L., Carter, A., Garzanti, E., Galy, V., Tabrez, A. R., Pringle, M., Campbell, I. H., France-Lanord, C., Blusztan, J., Allen, C., Alizai, A., Luckge, A., Danish, M. and Rabbani, M. M.: Monsoon control over erosion patterns in the

Western Himalaya: possible feed-back into the tectonic evolution., Geological Society, London, Special Publications, 342, 185-218,https://doi.org/10.1144/SP342.12, 2010.

Coutand, I., Barrier, L., Govin, G., Grujic, D., Hoorn, C., Dupont-Nivet, G. and Najman, Y.: Late Miocene-Pleistocene evolution of India-Eurasia convergence partitioning between the Bhutan Himalaya and the Shillong Plateau: New evidences from foreland basin deposits along the Dungsam Chu section, eastern Bhutan., Tectonics, 35,https://doi.org/10.1002/2016TC004258., 2016.

Coutand, I., Whipp, D. M. J., Grujic, D., Bernet, M., Fellin, M. G., Bookhagen, B., Landry, K. R., Ghalley, S. K. and Duncan, C.: Geometry and kinematics of the Main Himalayan Thrust and Neogene crustal exhumation in the Bhutanese Himalaya derived from inversion of multithermochronologic data., Journal of Geophysical Research, 119,https://doi.org/10.1002/2013JB010891, 2014.

DeCelles, P. G., Robinson, D. M., Quade, J., Ojha, T. P., Garzione, C. N., Copeland, P. and Upreti, B. N.: Stratigraphy, structure, and tectonic evolution of the Himalayan fold-and-thrust belt in western Nepal., Tectonics, 20, 487-509, 2001.

Diehl, T., Singer, J., Hetenyi, G., Grujic, D., Clinton, J., Giardini, D., Kissling, E. and group, G. W.: Seismotectonics of Bhutan: Evidence for segmentation of the Eastern Himalayas and link to foreland deformation., Earth and Planetary Science Letters, 471, 54-64,https://doi.org/10.1016/j.epsl.2017.04.038, 2017.

Drukpa, D., Velasco, A. A. and Doser, D. I.: Seismicity in the Kingdom of Bhutan (1937–2003): Evidence for crustal transcurrent deformation., Journal of Geophysical Research, 111,https://doi.org/10.1029/2004JB003087, 2006.

Duncan, C., Masek, J. and Fielding, E.: How steep are the Himalaya ? Characteristics and implications of along-strike topographic variations., Geology, 31, 75-78, 2003.

Fernandez-Blanco, D., de Gelder, G., Lacassin, R. and Armijo, R.: Geometry of Flexural Uplift by Continental Rifting in Corinth, Greece, Tectonics, 38,https://doi.org/10.1029/2019TC005685, 2020.

Forte, A. M. and Whipple, K. X.: Criteria and Tools for Determining Drainage Divide Stability., Earth and Planetary Science Letters, 493, 102-117,https://doi.org/10.1016/j.epsl.2018.04.026, 2018.

Gansser, A.: Geology of the Bhutan Himalaya, Birkhauser Verlag, Basel, Switzerland, 1983.

Gansser, A.: Geology of the Himalayas., Wiley-Interscience, New York (USA), 1964.

Gasparini, N. M., Whipple, K. X. and Bras, R. L.: Predictions of steady state and transient landscape morphology using sediment-flux-dependent river incision models., Journal of Geophysical Research, 112,https://doi.org/10.1029/2006JF000567, 2007.

Gautam, P. and Rösler, W.: Depositional chronology and fabric of Siwalik group sediments in Central Nepal from magnetostratigraphy and magnetic anisotropy., Journal of Geophysical Research, 17, 659-682, 1999.

Giachetta, E. and Willett, S. D.: Effects of river capture and sediment flux on the evolution of plateaus: indights from numerical modeling and river profile analysis in the Upper Blue Nile catchment., Journal of Geophysical Research, 123, 1187-1217,https://doi.org/10.1029/2017JF004252, 2018.

Godard, V., Bourlès, D. L., Spinabella, F., Burbank, D. W., Bookhagen, B., Fischer, G. B., Moulin, A. and Léanni, L.: Dominance of tectonics over climate in Himalayan denudation, Geology, 42, 243-246,https://doi.org/10.1130/G35342.1, 2014.

Godard, V., Cattin, R. and Lavé, J.: Numerical modeling of mountain building: Interplay between erosion law and crustal rheology, Geophysical Research Letters, 31,https://doi.org/10.1029/2004GL021006, 2004.

Goren, L., Willett, S. D., Herman, F. and Braun, J.: Coupled numerical–analytical approach to landscape evolution modeling., Earth Surface Processes and Landforms, 39, 522-545,https://doi.org/10.1002/esp.3514, 2014.

Govin, G., Najman, Y., Copley, A., Millar, I., van der Beek, P., Huyghe, P., Grujic, D. and Davenport, J.: Timing and mechanism of the rise of the Shillong Plateau in the Himalayan foreland., Geology, 46, 279-282,https://doi.org/10.1130/G39864.1, 2018.

Greenwood, L. V., Argles, T. W., Parrish, R. R., Harris, N. B. W. and Warren, C.: The geology and tectonics of central Bhutan., Journal of the Geological Society, 173, 352-369,https://doi.org/10.1144/jgs2015-031, 2016.

Grujic, D., Coutand, I., Bookhagen, B., Bonnet, S., Blythe, A. and Duncan, C.: Climatic forcing of erosion, landscape, and tectonics in the Bhutan Himalayas., Geology, 34, 801-804,https://doi.org/10.1130/G22648.1, 2006.

Guerit, L., Goren, L., Dominguez, S., Malavieille, J. and Castelltort, S.: Landscape 'stress' and reorganization from chi-maps: Insights from experimental drainage networks in oblique collision setting, Earth Surface Processes and Landforms, 43, 3152-3163,https://doi.org/10.1002/esp.4477, 2018.

Guillot, S. and Le Fort, P.: Geochemical constraints on the bimodal origin of High Himalayan leucogranites., Lithos 35, 221-234,https://doi.org/10.1016/0024-4937(94)00052-4, 1995.

Hammer, P., Berthet, T., Hetenyi, G., Cattin, R., Drukpa, D., Chophel, J., Lechmann, S., Le Moigne, N., Champollion, C. and Doerflinger, E.: Flexure of the India plate underneath the Bhutan Himalaya, Geophysical Research Letters, 40, 4225-4230,https://doi.org/10.1002/grl.50793, 2013.

Han, J., Gasparini, N. M. and Johnson, J. P. L.: Measuring the imprint of orographic rainfall gradients on the morphology of steady-state numerical fluvial landscapes, Earth Surface Processes and Landforms, 40, 1334-1350,https://doi.org/10.1002/esp.3723, 2015.

Han, J., Gasparini, N. M., Johnson, J. P. L. and Murphy, B. P.: Modeling the influence of rainfall gradients on discharge, bedrock erodibility, and river profile evolution, with application to the Big Island, Hawai'i, Journal of Geophysical Research - Earth Surface, 119, 1418-1440,https://doi.org/10.1002/ 2013JF002961, 2014.

Hasbargen, L. E. and Paola, C.: Landscape instability in an experimental drainage basin, Geology, 28, 1067-1070, 2000.

Hetenyi, G., Le Roux-Mallouf, R., Berthet, T., Cattin, R., Cauzzi, C., Phunthso, K. and Grolimund, R.: Joint approach combining damage and paleoseismol- ogy observations constrains the 1714 AD Bhutan earth- quake at magnitude 8 ± 0.5., Geophysical Research Letters, 43, 10695-10702,https://doi.org/10.1002/ 2016GL071033, 2016.

Hirschmiller, J., Grujic, D., Bookhagen, B., Coutand, I., Huyghe, P., Mugnier, J. L. and Ojha, T. P.: What controls the growth of the Himalayan foreland fold-and-thrust belt ?, Geology, 42, 247-250,https://doi.org/10.1130/G35057.1, 2014.

Hodges, K. V., Wobus, C. W., Ruhl, K., Schildgen, T. and Whipple, K. X.: Quaternary deformation, river steepening, and heavy precipitation at the front of the Higher Himalayan ranges, Earth and Planerary Science Letters, 220, 379-389,https://doi.org/10.1016/S0012-821X(04)00063-9, 2004.

Howard, A. D.: A detachment-limited model of drainage basin evolution, Water Resources Research, 30, 2261-2285,https://doi.org/10.1029/94WR00757, 1994.

Hubbard, J., Almeida, R., Foster, A., Sapkota, S. N., Burgi, P. and Tapponnier, P.: Structural segmentation controlled the 2015 Mw 7.8 Gorkha earthquake rupture in Nepal., Geology, 44, 639-642,https://doi.org/10.1130/G38077.1, 2016.

Huygue, P., Galy, A., Mugnier, J.L. and France-Lanord, C.: Propagation of the thrust system and erosion in the Lesser Himalaya: Geochemical and sedimentological evidence, Geology, 29, 1007-1010, 2001.

Iwata, S., Narama, C. and Karma: Three Holocene and late Pleistocene glacial stages inferred from moraines in the Lingshi and Thanza village areas, Bhutan, Quaternary International, 97-98, 69-78,https://doi.org/10.1016/s1040-6182(02)00052-6., 2002.

Lavé, J. and Avouac, J. P.: Fluvial incision and tectonic uplift across the Himalayas of central Nepal., Journal of Geophysical Research, 106, 26561-26591, 2001.

Le Fort, P., Cuney, M., Deniel, C., France-Lanord, C., Sheppard, S. M. F., Upreti, B. N. and Vidal, P.: Crustal generation of the Himalayan leucogranites, Tectonophysics, 134, 39-57, 1987.

Le Roux-Mallouf, R., Ferry, M., Cattin, R., Ritz, J.-F., Drukpa, D. and Pelgay, P.: A 2600-yr-long paleoseismic record for the Himalayan Main Frontal Thrust (Western Bhutan), Solid Earth,https://doi.org/10.5194/se-2020-59, 2020.

Le Roux-Mallouf, R., Ferry, M., Ritz, J.-F., Berthet, T., Cattin, R. and Drukpa, D.: First paleoseismic evidence for great surface-rupturing earthquakes in the Bhutan Himalayas., Journal of Geophysical Research, 121, 7271-7283,https://doi.org/10.1002/2015JB012733, 2016.

Le Roux-Mallouf, R., Godard, V., Cattin, R., Ferry, M., Gyeltshen, J., Ritz, J.-F., Drukpa, D., Guillou, V., Arnold, M., Aumaître, G., Bourlès, D. L. and Keddadouche, K.: Evidence for a wide and gently dipping Main Himalayan Thrust in western Bhutan., Geophysical Research Letters, 42,https://doi.org/10.1002/2015GL063767, 2015.

Liu, G. and Einsele, G. J. G. R.: Sedimentary history of the Tethyan basin in the Tibetan Himalayas., Geologische Rundschau, 83, 32-61, 1994.

Long, S., McQuarrie, N., Tobgay, T., Grujic, D. and Hollister, L.: Geologic Map of Bhutan, Journal of Maps, 7, 184-192,https://doi.org/10.4113/jom.2011.1159, 2011a.

Long, S., McQuarrie, N., Tobgay, T., Rose, C., Gehrels, G. and Grujic, D.: Tectonostratigraphy of the Lesser Himalaya of Bhutan: Implications for the along-strike stratigraphic continuity of the northern Indian margin, Geological Society of America Bulletin, 123, 1406-1426,https://doi.org/10.1130/B30202.1, 2011b.

Long, S. P., Mcquarrie, N., Tobgay, T., Coutand, I., Cooper, F. J., Reiners, P. W., Wartho, J.-A. and Hodges, K. V.: Variable shortening rates in the eastern Himalayan thrust belt, Bhutan: Insights from multiple thermochronologic and geochronologic data sets tied to kinematic reconstructions., Tectonics, 31,https://doi.org/10.1029/2012TC003155, 2012.

Lyon-Caen, H. and Molnar, P.: Constraints on the structure of the Himalaya from an analysis of gravity anomalies and a flexural model of the lithosphere, Journal of Geophysical Research, 88, 8171-8191,https://doi.org/10.1029/JB088iB10p08171, 1983.

Lyon-Caen, H. and Molnar, P.: Gravity anomalies, flexure of the Indian Plate, and the structure, support and evolution of the Himalaya and Ganga Basin, Tectonics, 4, 513-538,https://doi.org/10.1029/TC004i006p00513, 1985.

Marechal, A., Mazzotti, S., Cattin, R., Cazes, G., Vernant, P., Drukpa, D., Thinley, K., Tarayoun, A., Le Roux-Mallouf, R., Thapa, B. B., Pelgay, P., Gyeltshen, J., Doerflinger, E. and Gautier, S.: Evidence of interseismic coupling variations along the Bhutan Himalayan arc from new GPS data., Geophysical Research Letters, 43, 12399-12406,https://doi.org/10.1002/2016GL071163, 2016.

Matmon, A., Bierman, P. R., Larsen, J., Southworth, S., Pavich, M. and Caffee, M.: Temporally and spatially uniform rates of erosion in the southern Appalachian Great Smoky Mountains Geology, 31, 155-158,https://doi.org/10.1130/0091-7613(2003)031<0155:TASURO>2.0.CO;2, 2003.

McQuarrie, N., Robinson, D., Long, S., Tobgay, T., Grujic, D., Gehrels, G. and Ducea, M.: Preliminary stratigraphic and structural architecture of Bhutan: Implications for the along strike architecture of the Himalayan system, Earth and Planerary Science Letters, 272, 105-117,https://doi.org/10.1016/j.epsl.2008.04.030, 2008.

Meyer, M. C., Hofmann, C. C., Gemmell, A. M. D., Haslinger, E., Hausler, H. and Wangda, D.: Holocene glacier fluctuations and migration of Neolithic yak pastoralists into the high valleys of northwest Bhutan., Quaternary Science Reviews, 28, 1217-1237,https://doi.org/10.1016/j.quascirev.2008.12.025, 2009.

Mudd, S. M., Clubb, F. J., Gailleton, B. and D., H. M.: How concave are river channels ?, Earth Surface Dynamics, 6, 505-523,https://doi.org/10.5194/esurf-6-505-2018, 2018.

Perron, J. T. and Royden, L.: An integral approach to bedrock river profile analysis., Earth Surface Processes and Landforms, 38, 570-576,https://doi.org/10.1002/esp.3302, 2013.

Prince, P. S., Spotila, J. A. and Henika, W. S.: Stream capture as driver of transient landscape evolution in a tectonically quiescent setting, Geology, 39, 823-826,https://doi.org/10.1130/G32008.1, 2011.

Robinson, D. M., DeCelles, P. G., Patchett, P. J. and Garzione, C. N.: The kinematic evolution of the Nepalese Himalaya interpreted from Nd isotope, Earth and Planerary Science Letters, 192, 507-521, 2001.

Rosenkranz, R., Schildgen, T., Wittmann, H. and Spiegel, C.: Coupling erosion and topographic development in the rainiest place on Earth: Reconstructing the Shillong Plateau uplift history with in-situ cosmogenic 10Be, Earth and Planetary Science Letters, 483, 39-51,https://doi.org/10.1016/j.epsl.2017.11.047, 2018.

Sassolas-Serrayet, T., Cattin, R., Ferry, M., Godard, V. and Simoes, M.: Estimating the disequilibrium in denudation rates due to divide migration at the scale of river basins., Earth Surface Dynamics, 7, 1041-1057,https://doi.org/10.5194/esurf-7-1041-2019, 2019.

Schelling, D. and Arita, K.: Thrust tectonics, crustal shortening, and the structure of the far-eastern Nepal Himalaya, Tectonics, 10, 851-862, 1991.

Schwanghart, W. and Scherler, D.: Bumps in river profiles: uncertainty assessment and smoothing using quantile regression techniques., Earth Surface Dynamics, 5, 821-839,https://doi.org/10.5194/esurf-5-821-2017, 2017.

Schwanghart, W. and Scherler, D.: Divide mobility controls knickpoint migration on the Roan Plateau (Colorado, USA), Geology, 48, 698-702,https://doi.org/10.1130/G47054.1, 2020.

Schwanghart, W. and Scherler, D.: TopoToolbox 2 – MATLAB-based software for topographic analysis and modeling in Earth surface sciences, Earth Surface Dynamics, 2, 1-7,https://doi.org/10.5194/esurf-2-1-2014, 2014.

Simoes, M., Braun, J. and Bonnet, S.: Continental-scale erosion and transport laws: A new approach to quantitatively investigate macroscale landscapes and associated sediment fluxes over the geological past., Geochemistry Geophysics Geosystems, 11, Q09001,https://doi.org/10.1029/2010GC003121, 2010.

Simoes, M., Chen, Y.-G., Shinde, D. P. and Singhvi, A. K.: Lateral variations in the long-term slip rate of the Chelungpu fault, Central Taiwan, from the analysis of deformed fluvial terraces., Journal of Geophysical Research, 119,https://doi.org/10.1002/2013JB010057, 2014.

Singer, J., Kissling, E., Diehl, T. and Hetenyi, G.: The underthrusting Indian crust and its role in collision dynamics of the Eastern Himalaya in Bhutan: Insights from receiver function imaging, Journal of Geophysical Research, 122, 1152-1178,https://doi.org/10.1002/2016JB013337, 2017.

Stevens, V. and Avouac, J. P.: Interseismic coupling on the Main Himalayan Thrust., Geophysical Research Letters, 42, 5828-5837,https://doi.org/10.1002/2015GL064845, 2015.

Struth, L., Garcia-Castellanos, D., Viaplana-Muzas, M. and Verges, J.: Drainage network dynamics and knickpoint evolution in the Ebro and Duero basins: from endorheism to exorheism., Geomorphology, 327, 554-571,https://doi.org/10.1016/j.geomorph.2018.11.033, 2019.

Thiede, R. C., Arrowsmith, J. R., Bookhagen, B., McWilliams, M. O., Sobel, E. R. and Strecker, M. R.: From tectonically to erosionally controlled development of the Himalayan orogen, Geology, 33, 689-692,https://doi.org/10.1130/G21483AR.1, 2005.

Thiede, R. C., Bookhagen, B., Arrowsmith, J. R., Sobel, E. R. and Strecker, M. R.: Climatic control on rapid exhumation along the Southern Himalayan Front, Earth and Planerary Science Letters, 222, 791-806,https://doi.org/10.1016/j.epsl.2004.03.015, 2004.

Tobgay, T., Mcquarrie, N., Long, S., Kohn, M. J. and Corrie, S. L.: The age and rate of displacement along the Main Central Thrust in the western Bhutan Himalaya, Earth and Planetary Science Letters, 319-320, 146-158, 2012.

Tucker, G. E., Lancaster, S. T., Gasparini, N. M., Bras, R. L. and Rybarczyk, S. M.: An object-oriented framework for distributed hydrologic and geomorphic modeling using triangulated irregular networks., Computer Geosciences, 27, 959-973,https://doi.org/10.1016/s0098-3004(00)00134-5, 2001.

Upreti, B. N.: An overview of the stratigraphy and tectonics of the Nepal Himalaya., Journal of Asian Earth Sciences, 17, 577-606, 1999.

Verma, R. and Mukhopadhyay, M.: An analysis of the gravity field in northeastern India, Tectonophysics, 42, 283-317, 1977.

Viaplana-Muzas, M., Babault, J., Dominguez, S., Van Den Driessche, J. and Legrand, X.: Drainage network evolution and patterns of sedimentation in an experimental wedge., Tectonophysics, 664, 109-124,https://doi.org/10.1016/j.tecto.2015.09.007, 2015.

Viaplana-Muzas, M., Babault, J., Dominguez, S., Van Den Driessche, J. and Legrand, X.: Modelling of drainage dynamics influence on sediment routing system in a fold-and-thrust belt., Basin Research, 31, 290-310,https://doi.org/10.1111/bre.12321, 2019.

Whipple, K. X., DiBiase, R. A., Ouimet, W. B. and Forte, A. M.: Preservation or piracy: diagnosing low-relief, high-elevation surface formation mechanisms - Reply., Geology,https://doi.org/10.1130/G39252Y.1, 2017a.

Whipple, K. X., Forte, A. M., DiBiase, R. A., Gasparini, N. M. and Ouimet, W. B.: Timescales of landscape response to divide migration and drainage capture: Implications for the role of divide mobility in landscape evolution, Journal of Geophysical Research, 122, 248-273, 2017b.

Whipple, K. X. and Meade, B. J.: Controls on the strength of coupling among climate, erosion, and deformation in two-sided, frictional orogenic wedges at steady state, Journal of Geophysical Research, 109,https://doi.org/10.1029/2003JF000019, 2004.

Whipple, K. X. and Meade, B. J.: Orogen response to changes in climatic and tectonic forcing, Earth and Planerary Science Letters, 243, 218-228,https://doi.org/10.1016/j.epsl.2005.12.022, 2006.

Whipple, K. X. and Tucker, G. E.: Dynamics of the stream-power river incision model: implications for height limits of mountain ranges, landscape response timescales, and research needs., Journal of Geophysical Research, 104, 17661-17674,https://doi.org/10.1029/1999JB900120, 1999.

Willett, S. D.: Preservation or piracy: diagnosing low-relief, high-elevation surface formation mechanisms. - Comment, Geology,https://doi.org/10.1130/G38929C.1, 2017.

Willett, S. D. and Brandon, M. T.: On steady states of mountain belts, Geology, 30, 175-178, 2002.

Willett, S. D., McCoy, S. W., Perron, J. T., Goren, L. and Chen, C. Y.: Dynamic reorganization of river basins, Science, 343, 1248765,https://doi.org/10.1126/science.1248765, 2014.

Willett, S. D., Slingerland, R. and Hovius, N.: Uplift, shortening, and steady state topography in active mountain belts, American Journal of Science, 301, 455-485, 2001.

Yang, R., Willett, S. D. and Goren, L.: In situ low-relief landscape formation as a result of river network disruption., Nature, 520, 526-529,https://doi.org/10.1038/nature14354, 2015.

Yin, A., Dubey, C., Webb, A., Kelty, T., Grove, M., Gehrels, G. and Burgess, W.: Geologic correlation of the Himalayan orogen and Indian craton: Part 1. Structural geology, U-Pb zircon geochronology, and tectonic evolution of the Shillong Plateau and its neighboring regions in NE India., Geological Society of America Bulletin, 122, 336-359, 2010.